Sedimentology and carbon isotope stratigraphy of Lower–Middle Ordovician successions of Slemmestad (Oslo-Asker, Norway) and Brunflo (Jämtland, Sweden)

Olof Péterffy

Dissertations in Geology at Lund University,
Master's thesis, no 428
(45 hp/ECTS credits)

Department of Geology
Lund University
2015

Sedimentology and carbon isotope stratigraphy of Lower–Middle Ordovician successions of Slemmestad (Oslo-Asker, Norway) and Brunflo (Jämtland, Sweden)

Master's thesis

Olof Péterffy

Department of Geology
Lund University
2015

Contents

Cover Picture: The Hagastrand Member of the Tøyen Shale Formation at Bjerkåsholmen, Oslo-Asker.
Photo: Olof Peterffy

Sedimentology and carbon isotope stratigraphy of Lower–Middle Ordovician successions of Slemmestad (Oslo-Asker, Norway) and Brunflo (Jämtland, Sweden)

OLOF PÉTERFFY

Péterffy, O., 2015: Sedimentology and carbon isotope stratigraphy of Lower–Middle Ordovician successions of Slemmestad (Oslo-Asker, Norway) and Brunflo (Jämtland, Sweden). *Dissertations in Geology at Lund University*, No. 428, 41 pp. 45 hp (45 ECTS credits).

Abstract: Lower through Middle Ordovician strata are described with respect to sedimentology and carbon isotope stratigraphy from two areas, viz. two outcrops at Slemmestad in the Oslo-Asker district of southern Norway and a core section from the Brunflo area in Jämtland, central Sweden. The strata at these locations are compared and further correlation is done with the Tingskullen core section from Öland, south-eastern Sweden. Regionally important hardground complexes and beds such as 'Blommiga bladet' and 'Blodläget' and the 'Volkhov-Kunda boundary bed' are recognised in Jämtland and Slemmestad for the first time. The presented $\delta^{13}C_{carb}$-values from Slemmestad indicate subsequent diagenetic alterations, which hampers regional correlation of the Huk Formation. $\delta^{13}C_{org}$ from the Tøyen Shale Formation at this locality gives a more reliable signal and the BFICE has been tentatively recognised as 3.5 ‰ positive excursion in the uppermost part of the Hagastrand Member, although a higher data resolution would be needed to confirm it. The $\delta^{13}C_{carb}$ datasets from Brunflo and Tingskullen are both reliable and of high resolution. Several of the minor excursions and trends that characterise the generally stable carbon isotope record of the Lower and Middle Ordovician have been recognised, starting with the LTNICE, the BFICE, the Floian-Darriwilian rise and the BDNICE. A fast shift in the carbon isotope data is correlated to the 'Täljsten' interval which resents a regional biotic crisis. A negative excursion precedes the rising limb of the MDICE, which is clearly expressed (1.4 ‰) in the upper member of the Holen and Segerstad limestones in Brunflo. The correlation shows that the sedimentation rate was considerably higher in Slemmestad than in coeval strata in Jämtland and Öland during the Tremadocian and Floian; the Tremadocian is e.g. represented by almost 13 m of strata in Oslo as compared to the 2.5 m of coeval strata in Jämtland. The difference in sedimentation rate levelled out during the Dapingian and Darriwilian stages as a response to higher sea level at the time of deposition.

Keywords: Ordovician, carbon isotope stratigraphy, Baltoscandia, MDICE, 'Blommiga bladet', 'Blodläget'

Supervisors: Mikael Calner, Oliver Lehnert

Subject: Bedrock Geology

Olof Péterffy, Department of Geology, Lund University, Sölvegatan 12, SE-223 62 Lund, Sweden. E-mail: olofpeterffy@home.se

Sedimentologi och kolisotopstratigrafi avseende under- till mellanordoviciska avlagringar i Slemmestad (Oslo-Asker, Norge) och Brunflo (Jämtland, Sverige)

OLOF PÉTERFFY

Péterffy, O., 2015: Sedimentologi och kolisotopstratigrafi avseende under- till mellanordoviciska avlagringar i Slemmestad (Oslo-Asker, Norge) och Brunflo (Jämtland, Sverige). *Examensarbeten i geologi vid Lunds universitet*, Nr. 428, 41 sid. 45 hp.

Sammanfattning: Under- till mellanordoviciska avlagringar beskrivs med avseende på sedimentologi och kolisotopstratigrafi från två blottningar vid Slemmestad i Oslo-Askerdistriktet i södra Norge samt en borrkärnesektion från Brunfloområdet i Jämtland i Mittsverigeregionen. Avlagringarna från dessa platser jämfördes och korreleras med en borrkärnesektion från Tingskullen på Öland i sydöstra Sverige. Regionalt viktiga hårdbottenkomplex och bäddar, såsom Blommiga bladet, Blodläget och Volkhov-Kunda gränsbädden har påvisats i Jämtland och Slemmestad för första gången. De erhållna $\delta^{13}C_{carb}$-värdena från Slemmestad indikerar sentida påverkan av diagenetiska processer, något som inverkar negativt på Hukformationens regionala korrelationsmöjligheter. $\delta^{13}C_{org}$-data från Tøyenskifferformationen från den här lokalen ger en mer pålitlig signal och BFICE kan möjligtvis påvisas från lokalen som en 3,5 ‰ positiv exkursion i den övre delen av Hagastandledet, även om en högre datatäthet skulle behövas för att säkerställa att så verkligen är fallet. $\delta^{13}C_{carb}$-värdena från Brunflo och Tingskullen är både pålitliga och har hög uppläsning. Åtskilliga av de mindre exkursionerna och trenderna som kännetecknar den generellt sett stabila kolisotoputvecklingen i under– och mellanordovicium har påvisats, däribland LTNICE, BFICE, Floian-Darriwilianstigningen och BDNICE. En snabb skiftning i kolisotopdatan korreleras med Täljstensintervallet som representerar en regional biotisk kris. En negativ exkursion föregår den stigande delen av MDICE, som är tydligt utvecklad (1,4 ‰) i det övre ledet av Holenkalkstenen samt Segerstadkalkstenen i Brunflo. Korrelationen visar att sedimentationstakten var avsevärt mycket högre i Slemmestad än i motsvarande avlagringar från Jämtland och Öland under Tremadocian- och Floianfaserna; Tremadocianfasen representeras t.ex. av uppemot 13 m mäktiga avlagringar i Oslo, att jämföra med de 2,5 m mäktiga likåldriga avlagringarna i Jämtland. Skillnaden i sedimentationshastighet avtog emellertid under Dapingian- och Darriwilianfaserna som ett svar på högre havsnivå vid bildningstillfället.

Nyckelord: Ordovicium, kolisotopstratigrafi, Baltoskandia, MDICE, Blommiga bladet, Blodläget

Handledare: Mikael Calner, Oliver Lehnert

Ämne: Berggrundsgeologi

Olof Péterffy, Geologiska institutionen, Lunds universitet, Sölvegatan 12, 223 62 Lund, Sverige. E-post: olofpeterffy@home.se

1 Introduction

The Ordovician was in many respects a unique period in Earth history (Jaanusson 1984). With continents widely separated (Cocks 2001) and extensive ocean floor spreading, the ocean waters were pushed up on the continents. The unprecedentedly high sea levels allowed vast continental areas to be flooded by shallow seas (Barnes 2004; Munnecke et al. 2010). Biodiversity boomed (Sepkoski 1981; Webby et al. 2004). This interval in the history of life is critical to understand but interpreting the depositional history, sea level changes and depths of ancient epeiric seas can be challenging. Modern analogues are lacking and intellectual problems arise from, for instance, condensation and reworking of sediments (e.g. Burchette & Wright 1992; Wright & Burchette 1998). To untangle these issues a broad set of tools must be employed, including traditional facies analysis but also geochemical data (Munnecke et al. 2010). Reliable correlations are vital to differentiate local from regional to global events. Over the last years, carbon isotope chemostratigraphy has become a useful tool for correlational purposes (e.g. Bergström et al. 2009; Saltzman & Thomas 2012).

The present study focuses on Lower and Middle Ordovician sedimentary successions on the western margin of Baltica, more precisely, on the outcrops near Slemmestad in the Oslo-Asker district, Norway and on a core from Brunflo, Jämtland (Fig. 1). Carbon isotope stratigraphy on whole rock analysis will be presented from both successions, as well as isotope data from organic carbon in the Tøyen Shale Formation at Slemmestad, the first organic carbon study from the Lower Ordovician of this part of Baltoscandia.

While the global record of the Upper Ordovician features several well-studied high amplitude carbon isotope excursions, the Lower and Middle Ordovician is characterised by gentle isotopic shifts and a more subdued generalised curve (Bergström et al. 2009). The most prominent excursion in the Lower and Middle Ordovician is the mid-Darriwilian isotopic carbon excursion (MIDICE; e.g. Meidla et al. 2004; Ainsaar et al. 2010, Schmitz et al. 2010), but lately, several smaller scale excursions have been described from Baltoscandia (Lehnert et al. 2014). Four of these are of interest of the present study, namely the LTNICE (Late Tremadocian Negative Isotopic Carbon Excursion), BFICE (Basal Floian Isotopic Carbon Excursion, which marks the onset of the Floian-Darriwilian rise), BDNICE (Basal Dapingian Negative Isotopic Carbon Excursion) as well as the LDNICE (Lower Darriwilian Negative Isotopic Carbon Excursion). All of these have been recognised in the data presented from the Brunflo #2 core.

While sea level changes in the shallow, central parts of the basin may give rise to sharp facies shifts, large parts of the successions may also be cut out by erosion. The marginal marine strata provide a more complete stratigraphic record, even though any facies shifts related to sea level changes may be subtle. The aim of the present study is therefore to correlate these marginal deposits to the more central parts of the Baltoscandian basin in order to unravel the history of sea level changes at the time of deposition. A core recovered from Tingskullen on the island of Öland, Sweden, with a high resolution carbon isotope stratigraphy (Calner et al. 2014) linked to a detailed conodont biozonation by Wu et al. (submitted) will be used for comparison.

2 Geological setting

Three main physical aspects influenced environment and sedimentation in Baltica in the early Ordovician. The first of these was tectonically induced, as the continent was moving northwards across the southern hemisphere to higher latitudes with a warmer climate (Cocks & Torsvik 2005). This allowed the deposition of cold water carbonates in the Baltoscandian basin which hitherto in the Cambrian and lowermost Ordovician had been dominated by siliciclastic sedimentation (Calner et al. 2013). Secondly, the continent had been subject to a prolonged period of erosion and tectonic quiescence in the Precambrian, a process which had left the continent essentially flat and peneplanised (Lidmar-Bergstöm 1993, 1995). This had major consequences in combination with the third factor, namely the extraordinary high sea level.

Although the eustatic sea level fell somewhat in the Middle Ordovician, sea levels had risen since the Late Precambrian, and the Early Ordovician recorded the second highest sea level of the entire Palaeozoic (Nielsen 2004; Haq & Shutter 2008). In combination with the low relief, this allowed large parts of the continental surface to become inundated by a shallow epeiric sea. The low relief in itself, in combination with the drowning of source areas, led to extreme sediment starvation. Average net accumulation rates were merely 1–9 mm/1000 years in Sweden and the East Baltic area at the time, whereas the Oslo area had slightly higher values of 3–12 mm/1000 years, as it was located in the distal foreland of the Caledonides (Nielsen 2004). As a consequence, the Baltoscandian Cambrian to Middle Ordovician successions are relatively thin (Calner et al. 2013) and the entire Ordovician in Norway is represented by merely 400 m of strata (Bockelie 1982). Fluctuations in the relative sea level gave rise to the cyclic pattern displayed in the strata, with shale representing deeper conditions and limestone more shallow environments (Egenhoff et al. 2010).

The depositional and ecological environment in the basin varied with e.g. depth and distance from the coast line. Based on similarities in lithology and corresponding ecologic and faunal zonation, Jaanusson (1972, 1982, 1995) distinguished four 'Confacies Belts' in the Baltoscandian basin (Fig. 1A). The Scanian and Oslo belts are the most offshore of these, whereas the North Estonian with its southern counter-

part, the Lithuanian Confacies Belt represent the most nearshore conditions. The Central Baltoscandian Belt and its projection, the Livonian tongue, represent an intermediate position. The Oslo Confacies Belt distinguishes itself in having a broad variation in lithofacies and faunal composition, likely reflecting a pronounced bottom topography (Pärnaste et al. 2013), with the Oslo-Asker area situated in the deepest parts of the Oslo Confacies Belt (Fig. 2).

The 40-70 km wide and 115 km long Oslo Region (Oslofältet) preserves Lower Palaeozoic strata extending over an area of 10000 km^2 (Nakrem & Rasmussen 2013). The stratigraphic outline is presented in Figure 3. The Ordovician sedimentary successions of the Oslo Region have been studied by palaeontologists and sedimentologists for more than 150 years, with early contributions from e.g. Kjerulf (1857) and Brøgger (1882). Størmer (1953) outlined the regional lithostratigraphy and divided the region into different districts. The lithostratigraphy was subsequently thouroughly revised by Owen et al. (1990). The first general survey of the geochemistry of the strata was carried out by Bjørlykke (1974). Modern palaeontological studies include contributions by Ebbestad (1999; trilobites of the Bjørkåsholmen Formation), Nielsen (1995, trilobites of the Huk Formation), Hansen (2009, trilobites of the Elnes Formation), Rasmussen (1991, 2001; conodonts of the Huk Formation and coeval Stein Formation respectively) and Hoel (1999a,b; trilobites of the Tøyen Shale Formation).

The Oslo Region constituted a passive continental margin in the Cambrian and Early Ordovician, but with the incipient stages of the Caledonian Orogeny in the west during mid Darriwilian times (Elnes Formation) and onward, more siliciclastics were introduced into the basin (Bruton et al. 2010). At the peak of the orogeny in the Silurian, the successions were thrusted south-eastwards and folded; as a result, the studied successions in the Oslo Region dip steeply. Commonly, the Cambrian-Ordovician Alum Shale acted as a decollément plane (Bruton et al. 2010). Extension in the Permian further disturbed the successions both by the intrusion of dolerite dykes, as well as block faulting (Bockelie 1982); but if the succession had not been faulted down, they would have been eroded away and not be preserved today (Hansen et al. 2011). In other words, even when the boundaries of the preserved basin are those of a Permian aulacogen, the Early Palaeozoic sediments were originally deposited in an epicratonic basin (Owen et al. 1990).

Much like the Norwegian Early Ordovician successions, the Jämtland counterparts were also formed in a shallow epicontinental sea at the western, passive mar-

Fig. 1. A: Map of Baltoscandia with Lower Palaeozoic strata indicated. Confacies belts after Januusson (1995). B: Local map of the vicinity of Slemmestad. Field work was carried out at VEAS and Bjerkåsholmen C: Local map of Brunflo where the Brunflo #2 core was recovered.

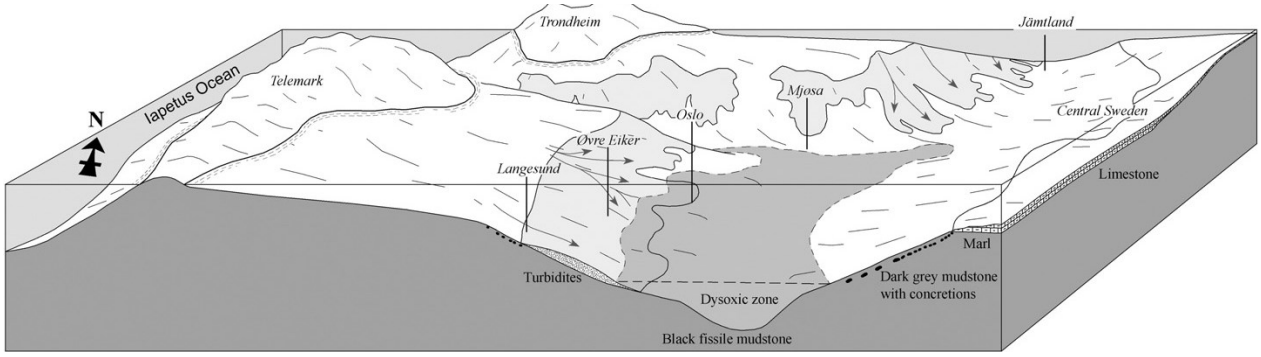

Fig. 2. Depositional environment of the Oslo Region during mid Darriwilian times (*Pterograptus elegans* graptolite Zone), i.e. after deposition of the Helskjer Member. Note that Jämtland was situated in slightly shallower environments than the Oslo area. From Hansen et al. (2011).

gin of Baltica that subsequently were subjected to deformation due to the Caledonian Orogeny (e.g. Karis 1998). Even though the Brunflo area is considered to be part of the autochthonous sequences of Jämtland, a minor degree of thrusting and faulting of the strata took place (Löfgren 1978). The Jämtland successions have been divided into a platform and ramp facies, where the Brunflo area constitutes the former because of the predominance of carbonate-dominated successions (Karis 1998). Accordingly, the palaeosetting is slightly shallower than the Slemmestad counterparts, and corresponds to the Central Confacies Belt (Fig. 1A, Fig. 2; Jaanusson 1995, Karis 1998).

The biostratigraphy of the Lower and Middle Ordovician of Jämtland is not particularily well known, but it has partly been studied with respect to conodonts (Löfgren 1978, Sturkell 1991), trilobites (Tjernvik 1956, Larsson 1973) and agnostids (Ahlberg 1988). Several reviews and excursion guides of the area have been published, including Bruton & Williams (1982), Karis (1998) and Wickström (2007). The stratigraphy is outlined in Figure 4.

3 Material and methods

Studies were undertaken in two successions which formed at the western margin of Baltica, the first represented by two outcrops in the vincinity of Slemmestad in Oslo-Asker and the other one recorded in a core recovered from the Brunflo area of Jämtland. More emphasis was put on the two outcrops in the former area (Fig. 1B). At the first outcrop, the beach at the Bjerkåsholmen peninsula, strata ranging from the Tremadocian part of the Alum Shale to the Darriwilian Svartodden Member of the Huk Formation are exposed. The Tøyen Shale Formation is only partly exposed. The succession is partly repeated at the second locality, a road cut at the Djuptrekkodden peninsula just 200 m to the north, also known as the VEAS section (Fig. 1B). The outcrop there includes the uppermost and tectonically deformed Tøyen Shale Formation, the entire Huk Formation as well as the basal part of the Elnes Formation.

The contemporaneous succession deposited at Brunflo, Jämtland (Fig.1C) was studied in the Brunflo #2 core which was drilled by the Geological Survey of Sweden (SGU) in 1970. The core section records autochtonous strata ranging from the Cambrian part of the Alum Shale Formation through a major part of the Lower-Middle Ordovician 'orthoceratite limestone', up to the Segerstad Limestone. The core, which is stored at the SGU office in Malå was sampled for carbon isotope chemostratigraphy by Rongchang Wu in early 2014 and further documented by the present author with respect to sedimentology in September 2014. These data was published in Wu et al. (in press) and are referred to below.

Field work was carried out at Slemmestad in May and October of 2014. At the later date the entire VEAS section had been thoroughly excavated, likely to reduce risk of slumping over the road. This has given new and relatively unweathered surfaces of the Huk Formation, but the Elnes Formation is now almost completely obscured at the locality. The sections were measured, logged and studied with respect to their macroscopical properties. The logs presented here are composite logs mainly based on the Bjerkåsholmen exposure, with the exception of the Svartodden Member and the Elnes Formation, which were logged at the VEAS section. The former unit is substantially better exposed at this locality after the excavation and the latter was logged prior to the excavation.

The lithology and faunal composition were studied using a polarised light microscope from about twenty thin sections that were prepared from rock samples collected at Bjerkåsholmen and the VEAS section. Furthermore, several rock samples were polished and examined using a standard optical microscope and a hand lens. Due to time constraints, no thin sections were prepared from the Brunflo #2 core, as a result only the latter method was employed. The sedimentological findings were then compared to the carbon isotope data of Wu et al. (in press) sampled in the same core.

A total of 106 samples for studies of bulk $\delta^{13}C_{carb}$ were collected from the limestone dominated formations at Slemmestad, i.e. the 10.6 m of strata that make up the Bjørkåsholmen and Huk formations as well as the exposed part of the Elnes Formation, yield-

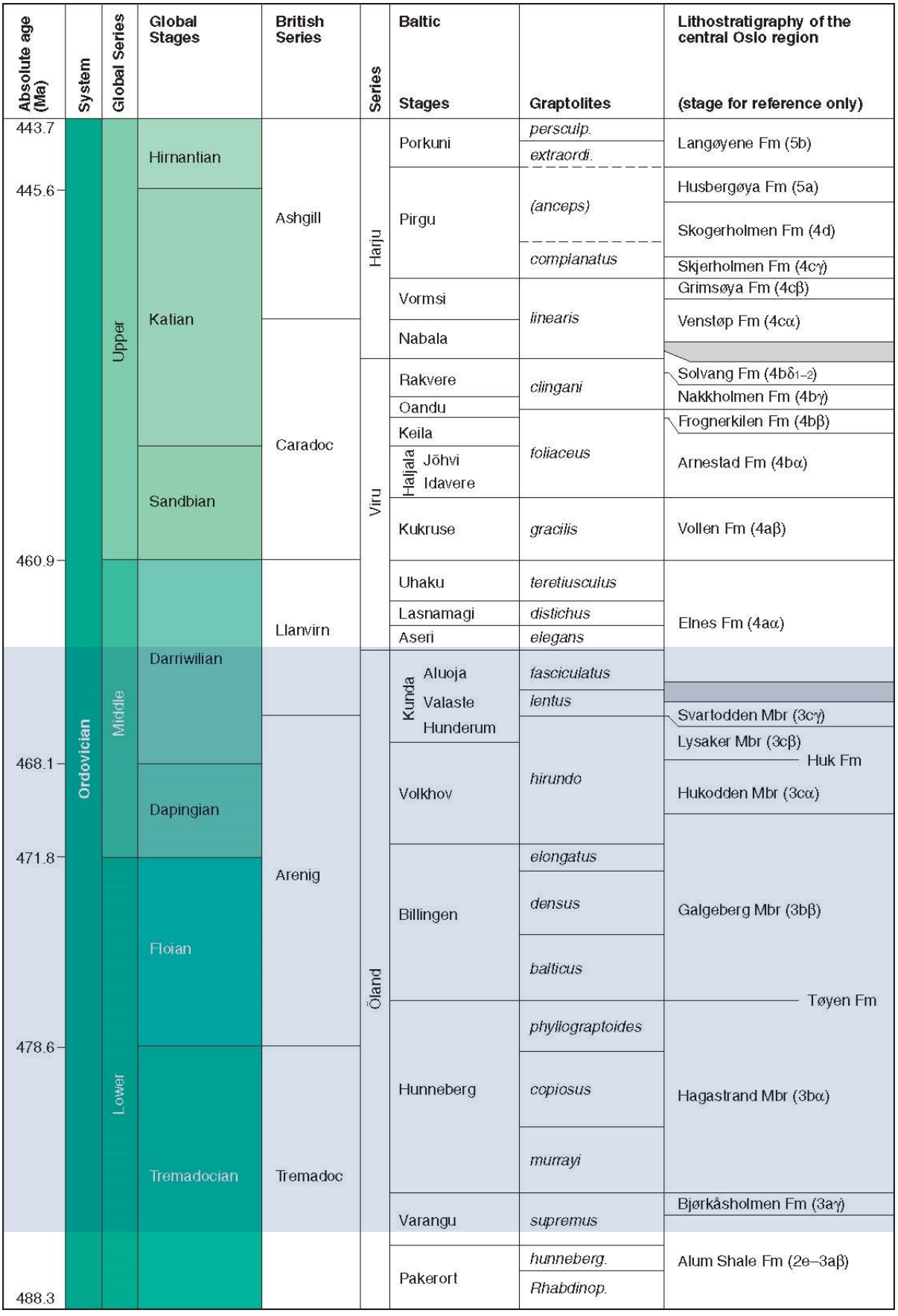

Fig. 3. Litho- and biostratigraphy of the central Oslo Region. From Nakrem & Rasmussen (2013), modified from Bruton et al. (2010). The interval studied in this thesis is marked by the blue box.

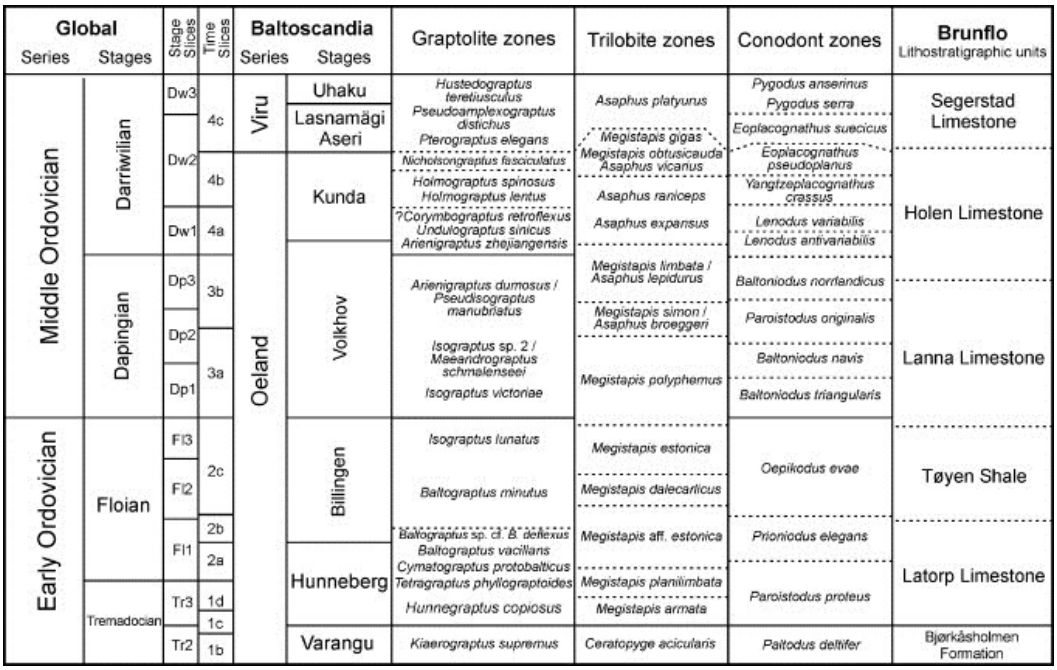

Fig. 4. Litho- and biostratigraphy of the Lower and Middle Ordovician strata in the Brunflo area. From Wu et al. (in press).

ing an average sampling density of one sample per 0.1 m. The first two formations were sampled at the Bjerkåsholmen peninsula and the latter at the Djuptrekkodden road cut. Samples were obtained using a micro-drill on fresh rock surfaces. Cement and calcite veins were avoided, and only micritic lithologies were targeted. Carbonate powders were subsequently reacted with 100% phosphoric acid (H3PO4) at 70 °C with a Gasbench II connected to a ThermoFinnigan Five Plus mass spectrometer. All reported values are in per mil relative to Vienna Pee Dee Belemnite (V-PDB) by assigning $\delta^{13}C$ and $\delta^{18}O$ values of +1.95‰ and −2.20‰ to the international standard NBS19 and −46.6‰ and −26.7‰ to the international standard LSVEC, respectively. Reproducibility and accuracy of carbon isotope analyses were monitored by replicate analysis of laboratory standards which were calibrated to NBS19 and LSVEC and were ±0.05‰ (±1 std. dev.).

Thirty-three samples for organic $\delta^{13}C$ studies were recovered from the 16.3 m of marine shales comprising the Tøyen Shale Formation, giving an average sampling density of about one sample per 0.5 m. Each sample was washed and then ground to a fine powder. 10 % hydrochloric acid was added after which the samples were allowed to react for several hours, a procedure which was repeated for the carbonate-rich samples several times. The acid was then decanted after which the samples were thoroughly washed with distilled water. Carbon isotope analysis of organic carbon was performed with an elemental analyser (CE 1110) connected online to a ThermoFinnigan Delta V Plus masspectrometer. All carbon isotope values are reported in the conventional δ-notation in permil relative to V-PDB. Accuracy and reproducibility of the analyses was checked by replicate analyses of international or laboratory standards (USGS 40 and Erl 5). Reproducibility was better than ±0,05 ‰ (1σ).

Analysis of elemental compositions was performed using scanning electron microscopy and EDX on glauconitic levels and levels with suspected pseudomorphs. Fresh rock samples were mounted in epoxy for easy handling and subsequently polished smooth using 1 micron diamond micropolish. The samples were carbon coated before analysis in a variable pressure Hitachi 3400N scanning electron microscope.

4 Stratigraphy

4.1 Slemmestad outcrops

The Bjerkåsholmen pensinsula and the VEAS section on Djuptrekkodden near Slemmestad, Oslo-Asker, exposes strata ranging from the upper Cambrian Alum Shale Formation to the middle Darriwilian Elnes formations. The strata dip steeply to the north-west and the formational boundaries are indicated in a detailed geological map (Fig. 5).

4.1.1 Alum Shale Formation

The Alum Shale Formation can be recognised over a vast area across the Baltoscandic platform, from Poland in the south to the East Baltic area in the east and even beneath the Caledonian nappes on the west coast of Norway (Gee 1980). It ranges stratigraphically from the middle Cambrian through the Tremadocian, its base being diachronous (Nielsen & Schovsbo 2007; Bruton et al. 2010 and references therein). The upper part of the shale unit in the Oslo Region is poorly fossiliferous, but has yielded specimens of the trilobite *Ceratopyge forficula* as well as the graptolites *Kiaerograptus kiaeri* and *Bryograptus ramosus* (Owen et al. 1990). Ebbestad (1999) assigns the top of the formation to the *Kiaerograptus supremus* graptolite Zone

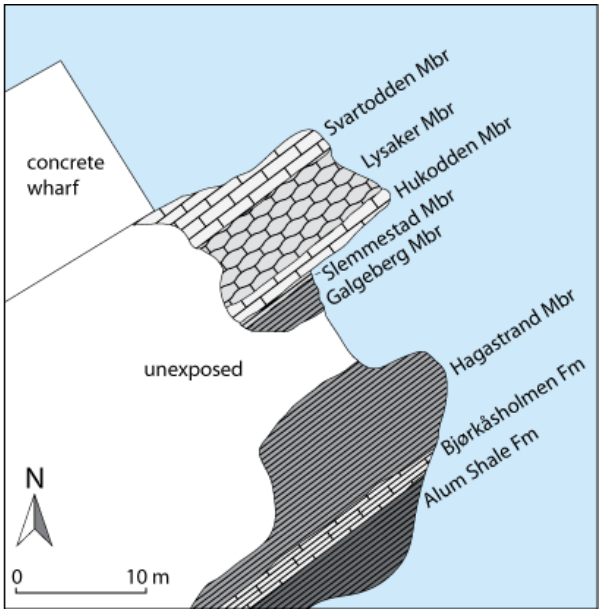

Fig. 5. Detailed map of the Bjerkåsholmen pensinsula where the almost vertically north-west dipping strata allow for good exposure of the sedimentary succession. The relative weathering resistance of the various lithologies is expressed by large scale geomorphology; the black shales represented by the Alum Shale and the Galgeberg Member coincide with bays, and the limestone-marl alternations of the Lysaker member also show a small indentation on the map. The Svartodden Member is bounded upwards by a fault contact at this locality.

of the Varangu Regional substage. The topmost part of the formation was previously known as the *Ceratopyge* Shale (Owen et al. 1990).

The Alum Shale Formation is severely deformed, displays prominent folds and is furthermore largely eroded away at Bjerkåsholmen. A detailed study of the formation is beyond the scope of this thesis. The black and highly kerogenous shales are poor in carbonate beds and carbonate concretions (or 'stinkstones') at Slemmestad and in the Oslo area (Owen et al. 1990). The lithology is fairly uniform, but the frequency of grey silt beds increases in the upper 0.6 m. A horizon with 2–3 cm long, black and ellipsoidal fine grained limestone concretions 0.06 m below the contact to the overlying Bjørkåsholmen Formation.

4.1.2 Bjørkåsholmen Formation

The 1.2 m thick Bjørkåsholmen Formation is widely distributed in the Oslo Region (e.g. Fjelldal 1966; Ebbestad 1999) and comprises microsparitic and micritic limestones with two thick shale interbeds (Figs. 6–7). Original depositional structures are hard to discern due to pervasive recrystallisation and diagenetic alterations (Fig. 8). The formation was formerly known as the Ceratopyge Limestone, but was redefined as the Bjørkåsholmen Formation by Owen et al. (1990).

Analysis of the trilobite faunas performed by Ebbestad (1999) shows that the thin unit spans the *Apatokephalus serratus* Zone. The basal nodular bed contains the *Ceratopyge* fauna, i.e. the fauna associated with *Ceratopyge forficula* and *Ceratopyge acicularis*. The top of the formation coincides with the top of the *Paltodus deltifer* conodont Biozone (Erdtmann & Paalits 1994).

The base of the formation is undulating and sharp, with a basal bed that constitutes wackestone nodules within a sparitic, recrystallised matrix (Fig. 1A,D). These pale grey nodules are well rounded but irregularly shaped, up to 0.2 m long, and some show signs of brittle deformation (Fig. 7A,B). Trilobite bioclasts dominate, but brachiopods and echinoderms also make up a substantial part of the fauna. Fine grained pyrite crystals (0.1 mm) are dispersed throughout the bed, but are more highly concentrated in the nodules.

The basal limestone bed is overlain by a 0.14 m thick dark grey shale bed that includes a layer of isolated black mudstone nodules. These nodules are dominated by the *Bienvillia angelini* olenid fauna and, as they can be traced throughout the Oslo region, the nodule layer acts as an important marker bed in the region (Ebbestad 1999).

The shale bed is succeeded by a 0.4 m massive set of six thin to medium thick limestone beds. This unit was named 'the main limestone bed' by Fjelldal (1966). The contact with the underlying shale is abrupt, and at the base black, well rounded limestone clasts occur again. These are macroscopically similar to those of the *Bienvillia angelini* bed but are here separated laterally by a 2–7 cm thick layer of fibrous crystalline calcite or orsten, resembling cone-in-cone structures (cf. Tucker 2001; Cobbold et al. 2013). The calcite fibres are conically arranged and crystal axes are oriented oblique to bedding. Calcite cone-in-cone

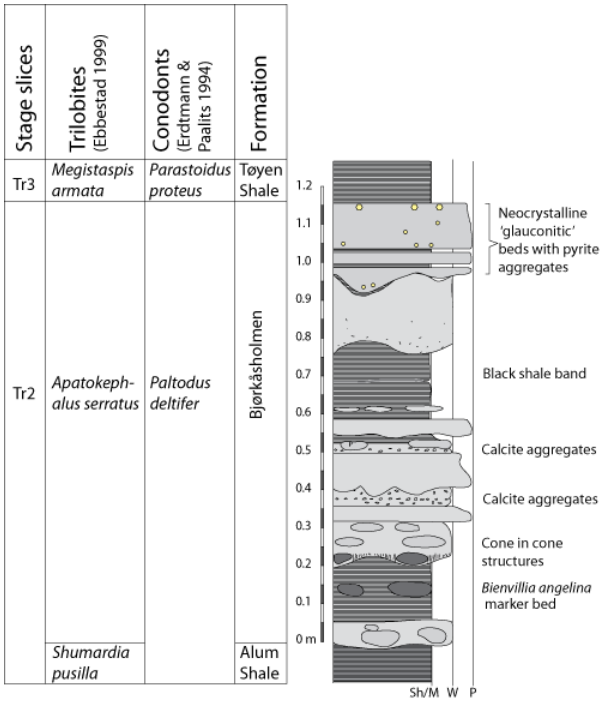

Fig. 6. Log of the Bjørkåsholmen Formation at Bjerkåsholmen in Slemmestad.

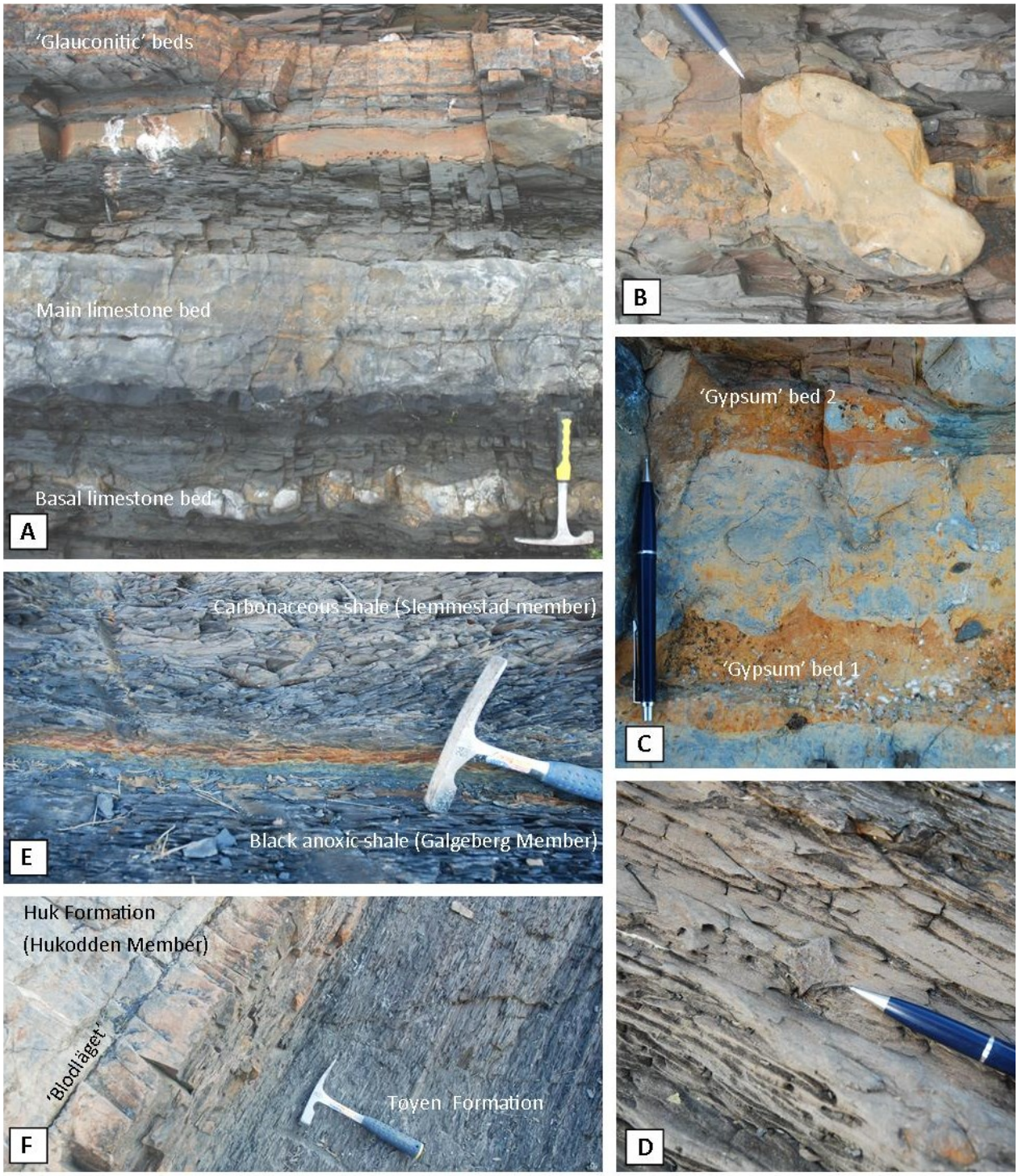

Fig. 7. Photographs of Bjørkåsholmen and Tøyen formations at Djuptrekkodden. A: The 1.2 m thick Björkåsholmen Formation in its entirety. B: Nodules (pale) set in a recrystallized matrix (orange) in the basal limestone bed of Bjørkåsholmen Fm. The upper nodule appears brittely deformed (at pen-tip). C: Two beds with white calcium carbonate crystal aggregates possibly representing pseudomorphs after gypsum, set in a recrystallized matrix. The grey middle bed is a wacke-packstone that has not undergone substantial recrystallisation D: Possible gypsum pseudomorph in the upper part of Hagastrand Member with conspicuous swallow-tail morphology. E: Multicoloured horizon at the base of the informal Slemmestad Member (Erdtmann 1965), possibly correlating with the 'Blommiga bladet' hardground. It is approximated as the base of the Dapingian in the section F: Contact between Tøyen and Huk formations.

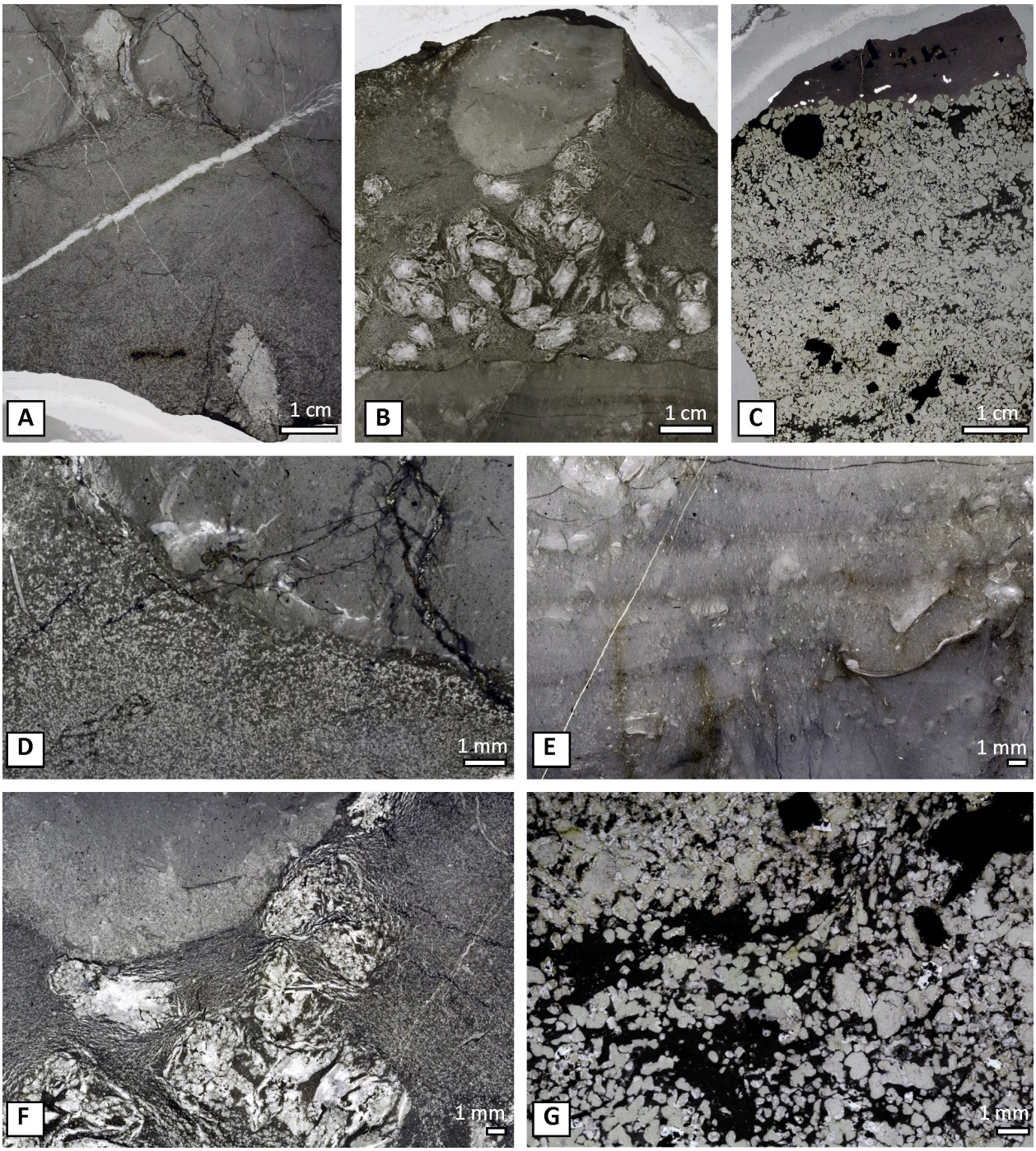

Fig. 8. Photomicrographs from the Björkåsholmen Formation. A: The basal bed shows trilobite wackestone nodules set in an almost thoroughly recrystallized matrix. A few trilobite grains have avoided recrystallisation. B: A bedding parallel laminated fabric is seen in the lower part. A sharp boundary divides this bed from the upper one which shows 1-2 cm long calcite aggregates which may represent gypsum pseudomorphs, set in a recrystallized matrix. Trilobite wackestone clast in the top. C: The uppermost bed of the Björkåsholmen Formation consists of crystal aggregates of uncertain affinity. Large opaque minerals are pyrite. Note cross-shaped pyrite crystal in the lower part, a shape indicative of replacement of gypsum. D: Close-up of (A), contact between recrystallized matrix and better-preserved nodule. E: Laminated lower part of (B). F: Close-up of upper part of (B). G: Close-up of (C). Note cross-shaped pyrite in upper right.

Table 1. Elemental composition of glauconite in the Bjørkåsholmen Formation.

Grain no.	Mg	Al	Si	K	O	Total
1	3.48	14.21	29.41	7.79	50.02	104.91
2	2.88	12.57	26.19	6.97	44.34	92.96
3	3.04	12.68	25.9	7.02	44.23	92.87
4	3.39	13.29	28.48	7.56	48.05	100.78
Mean	3.20	13.19	27.50	7.34	46.66	97.88

structures are commonly found in marine shales and are indicative of fluid overpressure during diagenesis (Cobbold et al. 2013).

Two beds (Fig. 6) feature conspicuous calcite crystals in ovoid or spherical shapes (Figs. 7C, 8B,E–F). Both of these beds are underlain by laminated wackestones. The calcite crystals seem to have grown in an unlithified, plastically deformed mud (Fig. 8B) and they have previously been interpreted as possible pseudomorphs of gypsum (Fjelldal 1966). The matrix itself show a gradation, with micrite in the upper part, transitioning to microspar in the middle part of the bed and down into pseudospar surrounding the ovoid crystals (Scholle & Ulmer-Scholle 2003, p. 270). Only few bioclasts occur in the sparitic matrix.

The 'main limestone bed' is capped by a thin bed of micritic packstone that does not show signs of recrystallisation. A ~0.2 m thick grey shale bed separates this unit from the topmost, ~0.4 m thick bedset of the formation. These beds are thoroughly recrystallised. The basal bed is a pale grey microsparitic mudstone with a few skeletal grains of mainly trilobites in its lower part. This horizon shows wavy bedding and varies in thickness from 0.1 to 0.3 metres.

The wavy bed is overlain by three thin and dark grey limestone bands, totalling 0.18 m in thickness. These beds are composed of sand sized, green aggregates set in a dark grey, cryptocrystalline quartz matrix. While the beds are entirely devoid of bioclasts, pyrite concretions are common and these occur both with framboidal morphology as well as twinned crosses (Fig. 8C,G). The twinned crystal habit is very similar to gypsum crystals documented in Scholle & Ulmer-Scholle (2003, p. 395), so the pyrite may well represent gypsum pseudomorphs. The green grains in these beds are irregular but rounded in shape, with radial cracks and have been interpreted as glauconite (e.g. Egenhoff et al. 2010). These grains are, however, not green in thin section (Fig. B10) and X-ray diffraction studies on glauconitic grains from Vestfossen and Bjerkåsholmen revealed only the presence of illite (Fjelldal 1966, Bjørlykke 1974). As a consequence Bjørlykke (1974) hypothesised that the grains were presumably glauconitic originally, but that they were diagenetically altered to illite. The chemical composition of these grains were analysed using EDX and the results are presented in Table 1. They have an average potassium content of 7.34%.

4.1.3 Tøyen Shale Formation

The Tøyen Shale Formation and its lithostratigraphic subdivision into three members was defined by Erdtmann (1965). The lowermost Hagastrand Member is characterised by grey shales and silty interbeds whereas the middle Galgeberg Member comprises dark, graptolitic shales. A third member, the Slemmestad Member, was also defined by Erdtmann (1965) for the uppermost part of the formation where the shales are paler and have a higher carbonate content. This member was subsequently discarded by Owen et al. (1990) however, as they considered this division was based on faunal rather than lithological differences.

The Tøyen Shale Formation is poorly exposed in the Oslo Region; the original stratotype section at Tøyen, Oslo where it was defined by Erdtmann (1965) was only briefly exposed during the construction of a railway tunnel. Therefore, Owen et al. (1990) designated a neostratotype at Engervik. These two publications, however, define the base of the Galgeberg Member differently. A level where graptolites appear defines the base of the Galgeberg Member according to Erdtmann (1965) whereas Owen et al. (1990) define the base of the Galgeberg Member where mudstone and gray shale interbeds cease. As Erdtmann based his division more on faunal rather than lithological basis, the definition by Owen et al. (1990) is preferred here.

The Tøyen Shale Formation is absent in the southern part of the Oslo Region, but can otherwise be recognised throughout the area (Owen et al. 1990). It also extends into Västergötland, Jämtland and Skåne in Sweden (e.g. volume by Bruton & Williams 1982). The unit is dominated by shales in the Oslo Region, but in Eiker-Sandsvaer, the Hagastrand Member is instead developed as a condensed, glauconitic limestone. Hoel (1999a) documented a diverse fauna of trilobites belonging to the *Megistaspis (Paramegistaspis) planilimbata* Zone in this facies. The biostratigraphy of the shaly facies is less well known; no recent biostratigraphical data from the Tøyen Shale Formation in Norway is known to the author. Furthermore, the Hagastrand Member is only sparsely graptolitic and Erdtmann (1965) found no graptolites at all in the lowermost 3 m. In contrast, the black shales of the overlying Galgeberg Member are rich in graptolites. Coinciding with the base of the member are the first appearances of *Tetragraptus approximatus* and *Tetragraptus phyllograptoides*, thus marking the base of the Floian stage (Cooper & Sadler 2012).

A total of 16.3 m of the Tøyen Shale Formation is exposed at the Bjerkåsholmen peninsula; the lower middle and middle part of the Galgeberg Member is obscured by Quaternary deposits (Fig. 5). Judging from the near-vertical dip of the strata and the distance between outcrops, the total thickness is estimated at 28 m, i.e. 8 m thicker than was described from the type locality at Tøyen, Oslo, by Erdtmann (1965). Tectonical thickening of the succession cannot be excluded.

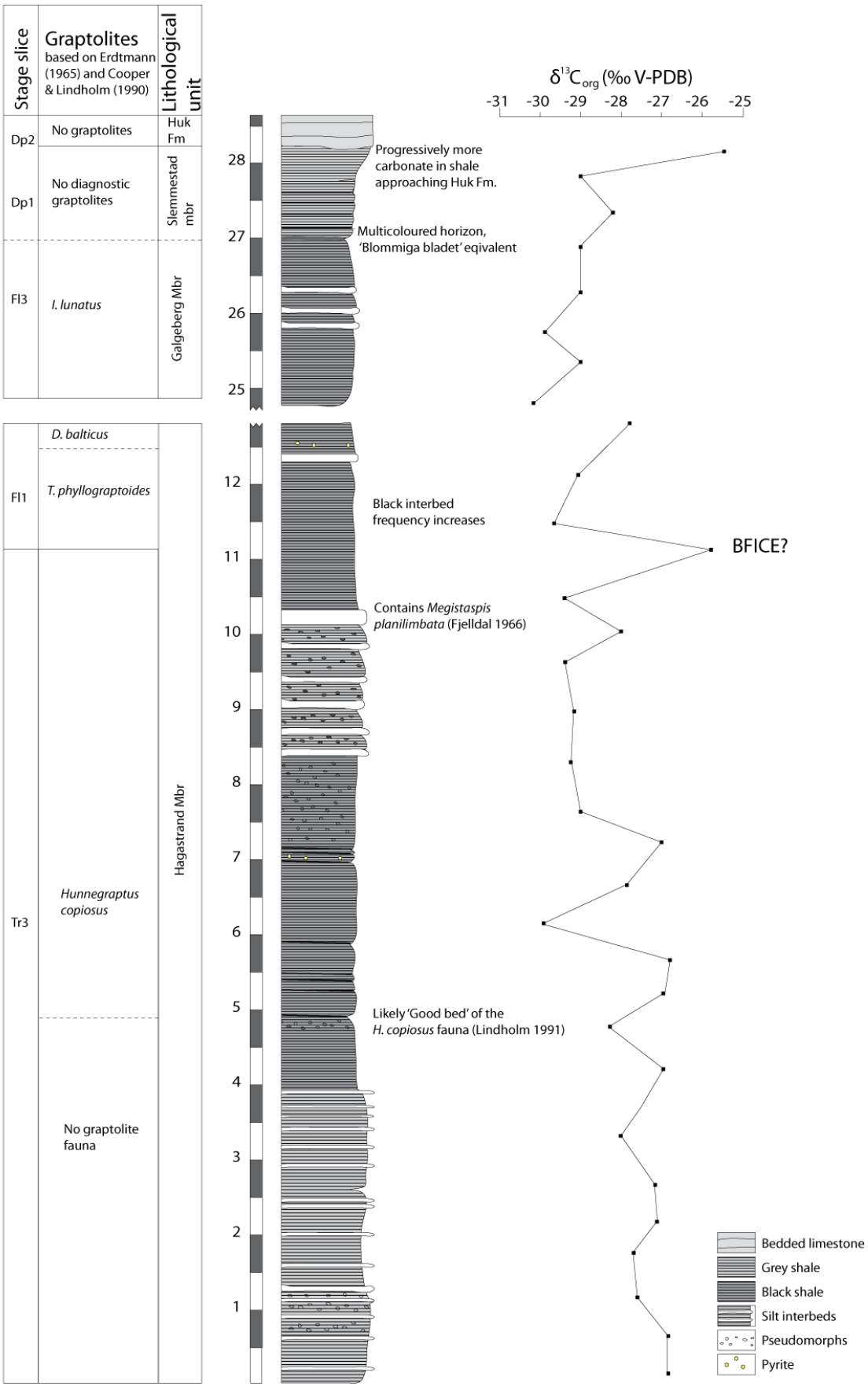

Fig. 9. Log of Töyen Shale formation at Djuptrekkodden in Slemmestad. Most of the Galgeberg Member is obscured by quaternary deposits at the locality due to the weathering prone black shale lithology.

The greenish 'glauconite' beds of the Bjørkåsholmen Formation end abruptly and is succeeded by the shales of the Hagastrand Member. Both the base and the top of the member are dominated by grey shales with calcareous mudstone interbeds whereas dark grey shales with black interbeds constitute the middle part (Fig. 9).

Rhytmically distributed, ~0.1 m thick beds, characterise the lowermost 4 metres of the formation. These are impure dolomitized mudstones, often containing large, up to 0.05 m long pyrite concretions arranged in bands.

About 1 m above the base, 5 mm large and often diamond shaped crystals and holes (from where the crystals have been weathered out) are common. They have been considered to represent pseudomorphs of gypsum, thus indicating evaporitic conditions (e.g. Erdtmann 1965). However, based on their shape and the high concentrations of barium in these beds, Antun (1967) and Bjørlykke (1974) suggested that they are pseudomorphs of barite (BaSO4). None of the presumed barite remains though, as it has been replaced by calcium carbonates, granular quartz and pyrite (Antun 1967). Therefore, the conclusion that these crystals originally represented barite (and not any other sulphate mineral) is by no means unambiguous.

Between ca 4 and 7 m above the base, the shales become more fissile than below, and black shales are interbedded in the grey shales. Silty interbeds are absent in this interval. Nonetheless, at 7 m pyrite aggregates (1-2 cm in diameter) can be observed, as well as holes that may either represent casts where the pyrite has been weathered out or possibly moulds of dissolved authigenic minerals.

An interval with grey shales with presumed pseudomorphs (Fig. 8D) and silty interbeds reappears at 8.45 m from the base of the formation, capped by a prominent 0.2 m thick mudstone bed. Above this bed, black and grey shale beds intercalations are observed and the lithology becomes progressively more black and fissile. Above a level of mudstone lenses at 12.3 m the strata are poorly exposed and covered by Quaternary deposits.

When comparing the observations of the present study with the log from Engervik by Owen et al. (1990), the base of the Galgeberg Member (including the informal, 1.3 m thick Slemmestad Member) at Bjerkåsholmen is inferred to be just above the level where the strata start to be obscured. In other words, the Galgeberg Member is not exposed in its entirety at Djuptrekkodden. The unexposed part of the member is estimated to be more than 12 m thick at the locality and 3.5 m of Galgeberg strata can be observed above the weathered out portion, just below the Huk Formation. Provided that the obscured strata are not folded or otherwise deformed, the thickness of the Galgeberg Member is up to 16 m thick.

The shales of Galgeberg Member above the obscured part are dark and fissile, but at 1.3 m below the base of the Huk Formation they culminate in a prominent pyrite impregnated horizon that shifts in bright colours ranging from blue-green to yellow to orange (Fig. 7E; see discussion for possible correlation). Above this level, the shales become progressively greyer and more carbonate rich (cf. Slemmestad Member as defined by Erdtmann, 1965).

4.1.4 Huk Formation

A sharp lithological change marks the transition from the Tøyen Shale Formation to the limestones of the Huk Formation, which is ca 8.5 m thick in the study area. The formation is part of the so called 'orthoceratite limestone', which has a wide distribution in Baltoscandia. The lithology shows a tripartite development in the Oslo Region and was divided into the Hukodden, Lysaker and Svartodden members by Owen et al. (1990). The basal and topmost members feature dark grey, compact limestones whereas the middle member is characterised by less weathering resistant limestone-marl alternations (Fig. 10). The formation's hypostratotype is located in Huk, Oslo-Asker.

4.1.4.1 Hukodden Member

The 1.7 m thick Hukodden Member comprises compact, greenish grey wacke- to packstones. The contact to the underlying Tøyen Shale Formation is distinct, a feature that is enhanced by weathering of the less resistant shales (Fig. 7F).

The basal beds show a wide lithological variation and call for a more detailed description. The basal 10 cm are made up of a thoroughly recrystallised mudstone with few remaining skeletal clasts. The lowermost centimetre displays a slight fissility, reflecting a certain amount of terrigenous material in the basal lime mudstone. Above this interval the shale content decreases rapidly, but the rock becomes progressively darker, culminating in a dark band 5 cm from the base. This layer likely reflects a higher content of organic material. Dark structures that may represent burrows extend upwards and downwards from this band, and in places the burrows can also be traced laterally. These traces have a flattened appearance, suggesting post-compressional lithification. Above this horizon the limestone shows the same recrystallisation as below, but is substantially paler.

A boundary, which appears at 0.1–0.13 cm from the base of the formation, separates the recrystallised rock from a dense trilobite and brachiopod packstone. The dark grey mineralised zone is 5 mm thick and has a sharp, well defined top but a gradual base. Laterally, the contact is undulating but smooth, and shows no signs of boring. The packstone bed above this zone is only 4 cm thick and is capped by a prominent hardground, 0.17 m above the base (Fig. 11A–B). The irregular surface is impregnated by millimetre-sized pyrite cubes and narrow cylindrical borings extending up to 3 cm below the surface. According to Rasmussen (1991, p. 267) and Rasmussen et al. (2013), this sur-

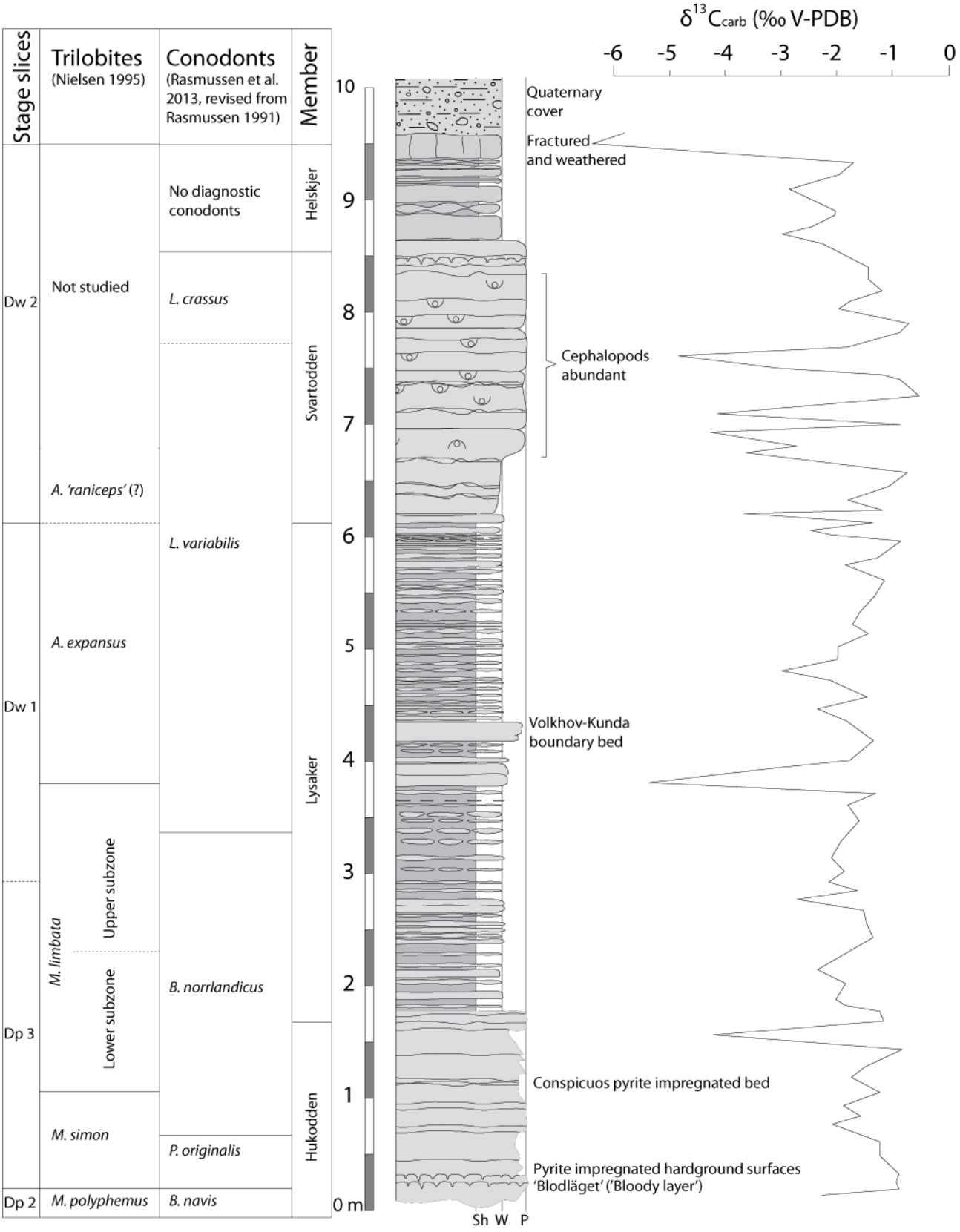

Fig. 10. Composite log of Huk Formation at Djuptrekkodden and the VEAS section with carbon isotope data from the limestones, displaying a diagenetic overprint of the strata. The Huk Formation shows a clear lithological differentiation between the three members; the Hukodden and Svartodden members are dominated by compact wacke-packstones whereas the Lysaker Member is characterized by rhythmic limestone-marl interbeds.

face represents a hiatus spanning from the middle *Baltoniodus navis* to the basal *Paroistodus originalis* conodont biozones). Furthermore, it marks the boundary between the *Megistaspis polyphemus* and *Megistaspis simon* trilobite zones (Nielsen 1995; Fig. 10). This makes it coeval with 'Blodläget', a hardground complex developed as a bed of three hematite impregnated surfaces on Öland, where it also marks the base of the *Parastoidus originalis* Biozone (Lindström 1979; see discussion).

Above this hardground, the lithology is dominanted by bioturbated wackestone-packstone. Dark blue grey patches of packstone with grains oriented parallel to the bedding are separated by centimetre-thick greenish wackestone areas. These have a more chaotic fabric and likely represent burrows, with a bioturbation index of 4 (*sensu* Droser & Bottjer 1986). Bioclasts (mainly trilobites, but also brachiopods and echinoderms) are bored and fragmented (Fig. 12A–B).

A well-defined pyrite impregnated lamina is present at 0.24 m above the formational base, and less distinct ones occur at regular intervals up to 1.0 m above the base of the formation, where three conspicuous anastomosing pyrite laminae are developed (Fig. 11B–C). These coincide with the *M. simon/Megistaspis limbata* zonal boundary (Nielsen 1995). Bedding planes in the middle part of the member are marked by thin, undulating clay seams. In the uppermost 0.2 m of the unit are these are instead developed as up to centimetre thick marls (Fig. 11D).

The lithology alternates between wackestone and packstone, comprising a mixed facies as defined by Harris et al. (2004), indicating a depositional setting in the middle shelf. This is concordant with the ichnofabric where the bioturbation index, as well as the ubiquitous bored skeletal clasts, suggests a low sedimentation rate and a high degree of reworking. Conodont studies by Rasmussen (1991) shows considerably higher conodont element densities (up to 700 specimens/0.7 kg) in the lower half than in the upper part of the member (approx. 50 specimens/0.7 kg), suggesting a higher degree of condensation in the lower part.

Marl beds are introduced in the upper part of the unit, showing a gradual transition to the overlying Lysaker Member. Therefore, the transition between the lithologically distinct units is not interpreted to be associated with any significant hiatus, but indicates that the sedimentological conditions gradually changed. Nonetheless, it must be stressed that the facies shift between the two units is substantial (Fig. 11D).

The greenish tint indicates reducing conditions during early diagenesis (Jaanusson 1972). The grey colour also reflects high contents of organic carbon. When little oxygen is available, the organic material is not fully decomposed and is thus retained in the sediments.

4.1.4.2 Lysaker Member

The 4.4 m thick Lysaker Member comprises rhytmically stacked limestone beds intercalated with thin marl beds. The strata belong to the *Megistaspis limbata* and *Asaphus expansus* biozones (Nielsen 1995). Wavy, parallel beds of mainly wackestone dominate generally but lenticular, subparallel beds make up the upper lower half of the member (Figs. 10,12C–D). Individual beds range in thickness from 0.01 to 0.2 m. The thickest bed is found at 2.0 m above the base of the formation, a packstone bed which is also characterised by having a coarser grain size than the rest of the formation. It coincides with the transition between *M. limbata* and *A. expansus* trilobite zones (Nielsen 1995), a level which has been suggested to represent a sea level fall in Baltoscandia at the Volkhov-Kunda transition (Lindskog et al. 2014; see discussion).

As noted by Rasmussen (1991), carbonate beds dominate the lithology in the lowermost, middle and uppermost part of the unit, whereas the strata in between these levels are more nodular and dominated by shale. The beds are stacked in a cyclic pattern and thicknesses of individual carbonate beds range in between 1 and 20 cm, but the thicker ones are cut by dissolution seams.

Trilobites and brachiopods represent important constituents of the fauna, but echinoderms and bryozoans are more important in the Lysaker Member than in the underlying Hukodden Member.

4.1.4.3 Svartodden Member

The rhythmic beds of the Lysaker Member are contrasted by the compact dark grey limestones of the overlying Svartodden Member (Fig. 13A). Biostratigrapically, the base of the Svartodden Member belongs to the *Lenodus variabilis* zone while the top yields conodonts of the *Lenodus crassus* zone (Rasmussen et al. 2013). The unit is homogenous at first glance, but shows a variation in faunal and lithological composition upon closer inspection; the unit is relatively fine grained in the lowermost 0.5 m, being dominated by wackestones. Above this interval, packstone makes up the lithology and endoceratiid conches are common, especially in the mid-upper part.

The basal 0.2 m thick bed constitutes a wackestone with *Thalassinoides* burrows. Brögger (1882) noted characteristic, millimetre sized lenticular phosphorite grains and dubbed this the '*Porambonites* bed' due to its high content of this brachiopod.

Endoceratids appear for the first time at 0.6 m above the base of the member and are frequent up to 2.15 m from the base (Figs. 10,13B. These conches frequently show signs of dissolution in their upper half, and these omission surfaces indicate that the water was not saturated with respect to calcium carbonate. Siphuncles are often, but not always oriented way down (Fig. 13C).

Whereas Hansen (2011) interpreted the Svartodden Member as shallow water deposits, well in the reach of storm waves but not quite above fair weather wave base, Nielsen (2004) considered these pure limestones to be the product of a drowning event that shut off

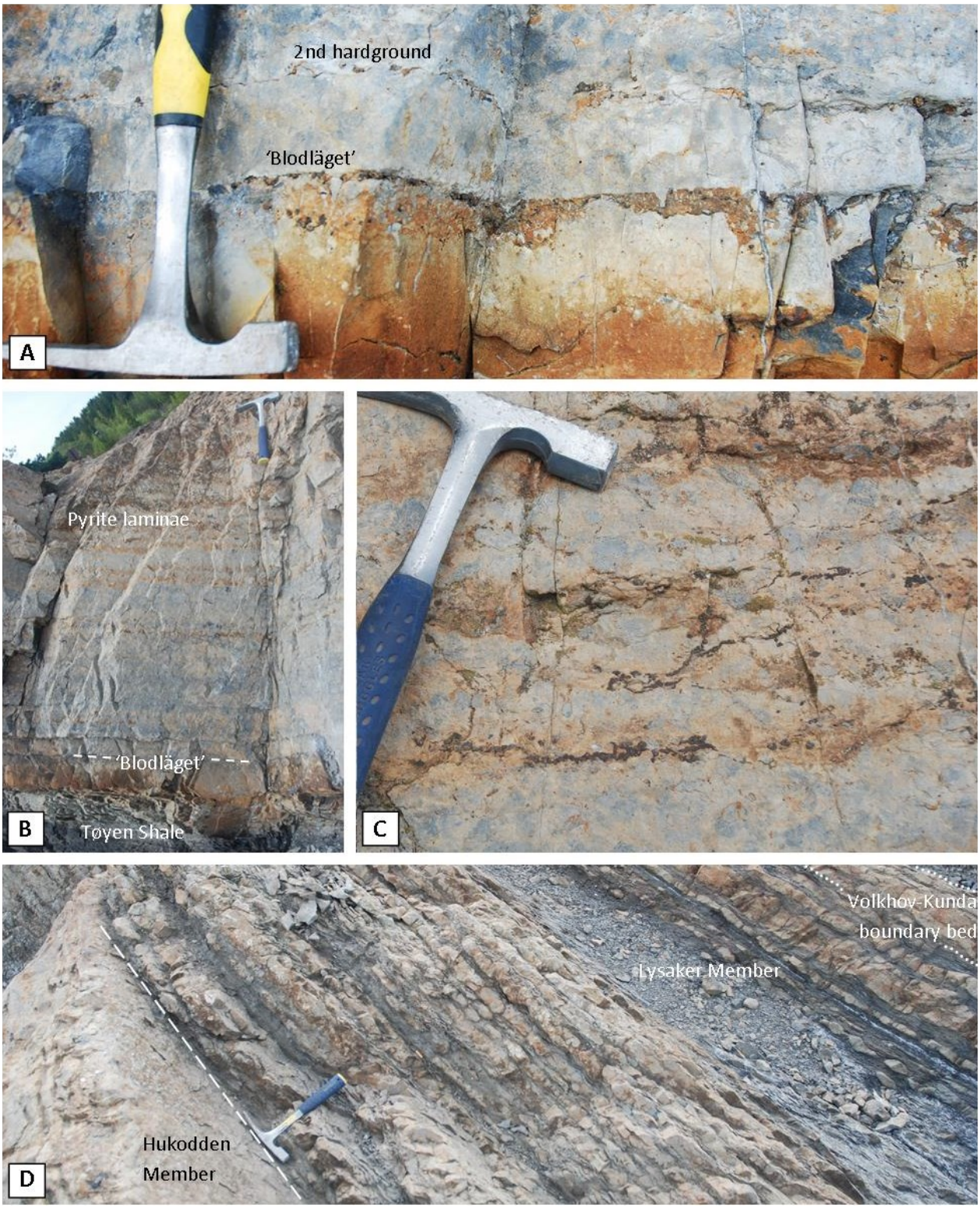

Fig. 11. Hukodden and Lysaker members. A: Twin hardgrounds near the base of the Hukodden Member. B: Overview of the massive limestones of the Hukodden Member. C: Conspicuous pyrite impregnated laminae in the middle of the Hukodden Member, marking the base of M. limbata Zone (Nielsen 1995). D: The Lysaker Member is characterized by lime-marl alterations, with the more nodular facies to the right being more prone to erosion. Stratigraphic up is to the right. The Volkhov-Kunda boundary bed is visible in the top right corner.

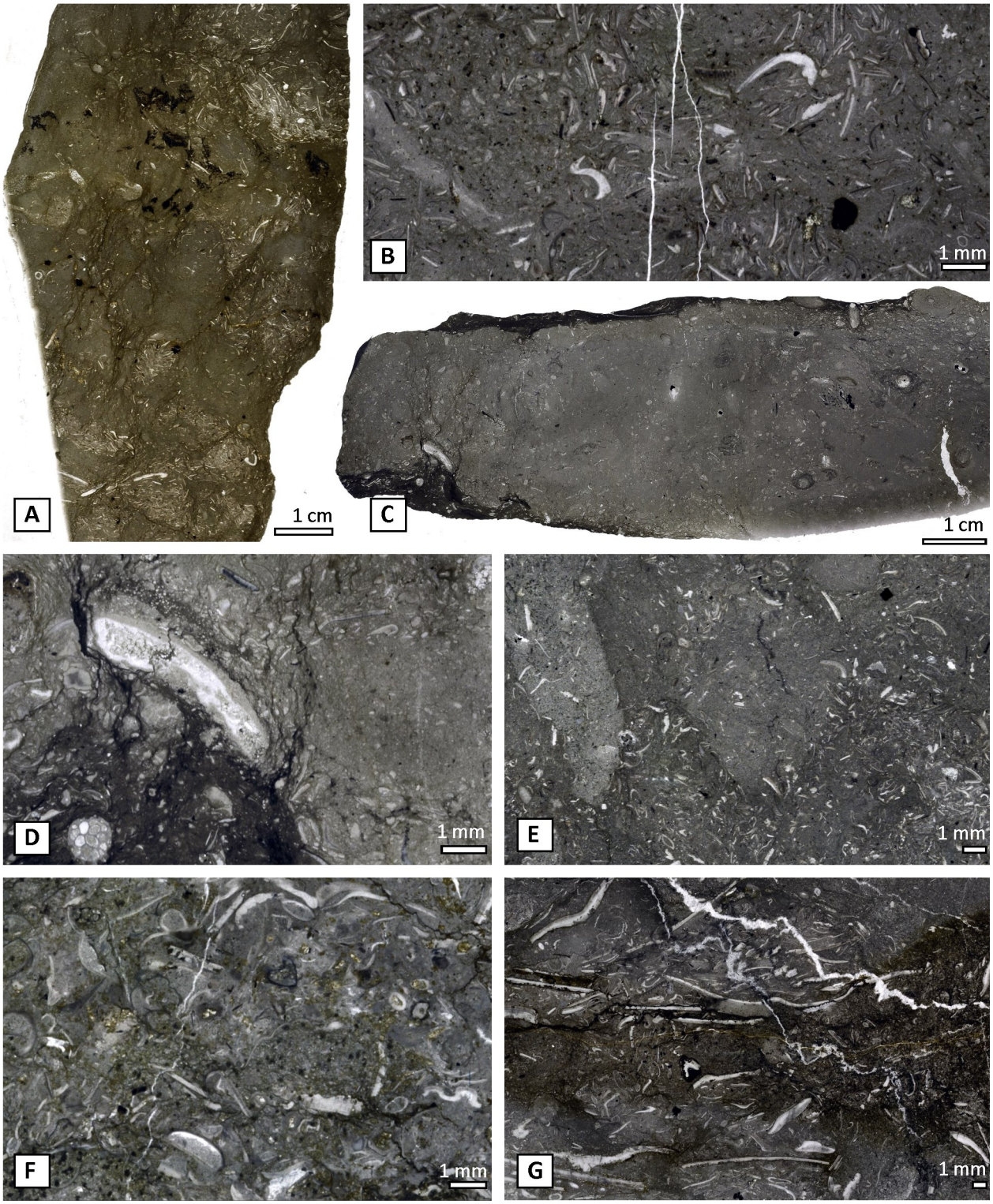

Fig. 12. Photomicrographs from the Huk and Elnes formations. A: Trilobite wackestone with pockets of packstone, Hukodden Member. Packstone shells are unbroken, in contrast to those of the wackestone B: Wacke- and packstone, Hukodden Member. Ubiquitous fine grained pyrite. C: A lime-band of the Lysaker member of trilobite and echinoderm wackestone. D: Close-up of (C). Note shell fragments also in marly, lower left part. E: Well sorted and bioturbated trilobite wacke-packstone, Svartodden Member. F: Trilobite and echinoderm packstone, Svartodden Member. G: Trilobite wackestone, Helskjer Member (Elnes Formation). Note abundance of bored bioclasts.

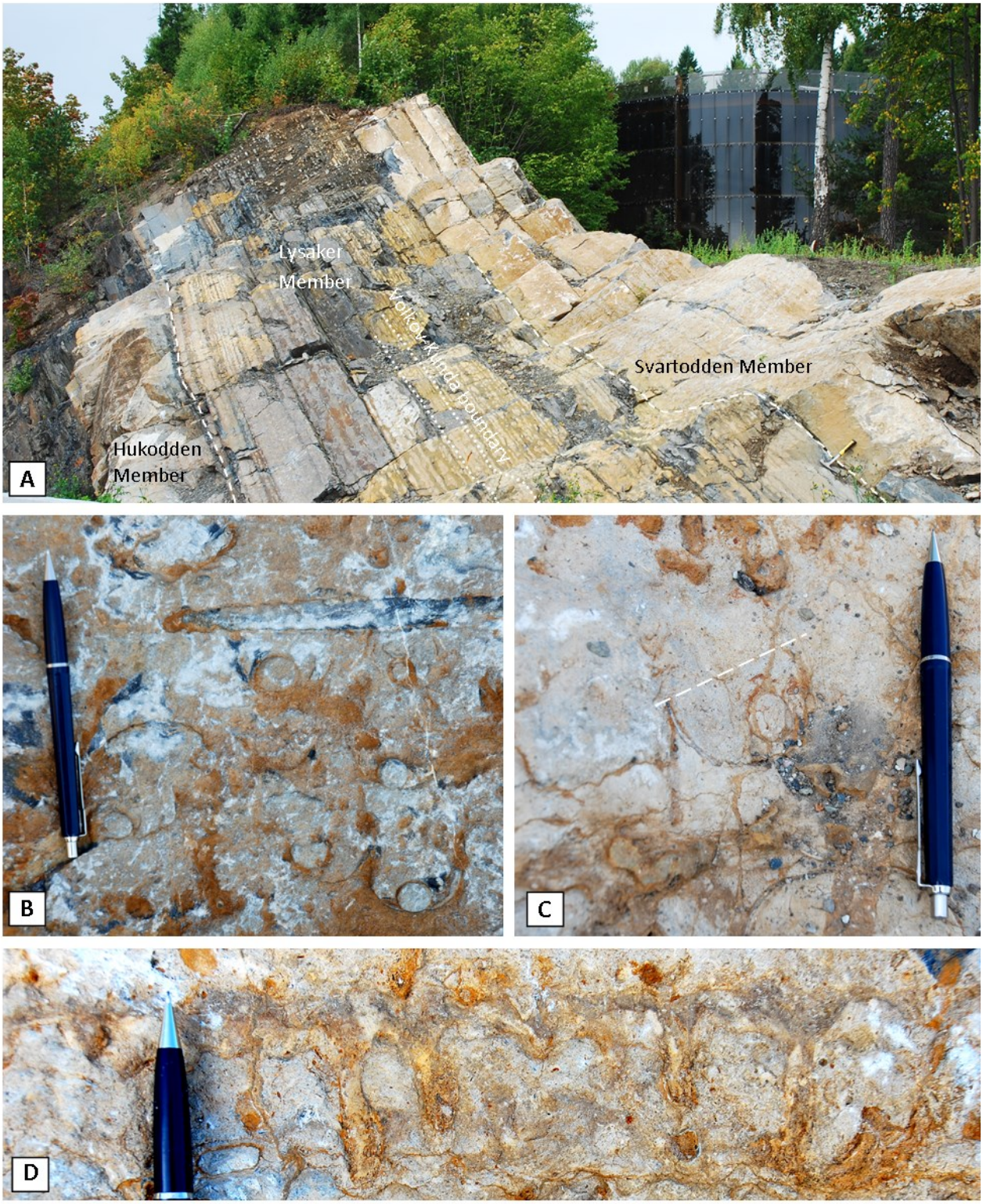

Fig. 13. The recently re-excavated VEAS section at Djuptrekkodden peninsula, note hammer for scale. The tripartite development of the Huk Formation is very well expressed. B: The compact packstones of the Svartodden Member feature abundant endoceratids with omission surfaces. C: The omission surface of this endoceratid is arranged obliquely to bedding, indicating post-depositional disturbance. D:Hardground with amphora-like borings near the top of the Svartodden Member.

clastic supply. The often well sorted sediments, the coarse grain size and the low degree of lime mud in the middle and upper parts (Fig. 12E) support the former opinion. Indicative of a depositional setting below fair weather wave base is the fact that most, but not all, nautoidal siphuncles are arranged close to bottom position. This suggests that the conches were undisturbed by wave action at least until they had time to become securely fastened by surrounding sediment (Reyment 1968).

A facies shift is seen 0.3 m below the top of the formation. This part does contain a few endoceratids but is characterised by frequent stylolites. These occur at regular, approximately 3 cm, intervals and show amplitudes of 1–3 cm. In this interval, more precisely at 2.35 m above the base of the member, a possible hardground is developed (Fig. 13D). It is not heavily mineralised, but feature frequent amphora-like borings with narrow necks (cf. *Trypanites*), extending typically 4 cm below the surface.

4.1.5 Helskjer Member (Elnes Formation)

The basal metre of the Helskjer Member was exposed at the VEAS road cut, but only very poorly so after the re-excavation during the summer 2014. The lithology makes the unit susceptible to erosion: wavy bands and nodules of limestone interbedded with marls. The bioclast content is dominated by bored trilobite shells, but echinoderms and brachiopods also contribute. The basal part of the formation is composed of wackestones, but bioturbation is visible as channels filled with packstone (Fig. 12F–G). Higher up, they grade into a more fine grained facies, characterised by mud to wackestones with only small and highly fragmented bioclasts.

The strata display a general fining upward trend, with a mixed wacke-packstone facies at the base of the unit and a mud supported facies seen in the upper part. The Helskjer Member is also overlain by the black shales of the Sjøstrand Member (Owen et al. 1990, Hansen 2009). Overall, this facies association indicates a transgressive development during the time of deposition.

4.2 Brunflo #2 core

The Brunflo #2 core was recovered by the Swedish Geological Survey in 1970 and preserves strata ranging from the Furongian Alum Shale to the Darriwilian Segerstad Limestone (Fig. 14).

4.2.1 Ceratopyge Limestone

The Ordovician strata of the Brunflo core start with the Ceratopyge Limestone, a thin glauconite-enriched unit which is separated from the underlying Cambrian limestones by a sharp discontinuity surface at -41.20 cm. The topmost Cambrian limestone in the core yields abundant olenid trilobite fragments that can be assigned to the Jiangshanian Stage (Wu et al. in press). Conodont studies performed in the Brunflo area by Sturkell (1991) indicated that Ceratopyge Limestone belong to the upper *Paltodus deltifer* zone, corresponding to the Tr2 stage slice (Pärnaste et al. 2013). In other words, a substantial hiatus is inferred between the Cambrian and Ordovician strata.

The Ceratopyge Limestone is only 0.05 m thick and was first recognised as a separate formation in the area by Sturkell (1991). The formation comprises two thin glauconitic beds (Fig. 15A), representing wackestone to packstone dominated by vermicular and fractured glauconite grains. The lowermost bed is also rich in trilobite and brachiopod skeletal clasts as well as a few pyrite grains. In contrast, the upper bed is completely devoid of bioclasts and the glaucony takes on a significantly darker green colour. The beds are separated by a distinct but irregular surface. A darker green colour indicates higher maturity of the glauconite in the upper bed (Odin & Matter 1981); this conclusion is supported by the performed SEM-studies (Table 2). Potassium content is high in the glaucony of both beds; the lower bed has an average content of 9.03% K, while the upper bed has a slightly higher average content; 9.40%.

The glauconitic minerals in the Caratopyge Limestone are fractured. This feature indicate (although not unequivocally) an autochtonous origin of the grains, as these otherwise would break along these weakness zones (Amorosi 1997). Nonetheless, a certain degree of reworking is inferred by the findings of abraded conodont elements (Sturkell 1991).

4.2.2 Latorp Limestone

The 2.5 m thick Latorp Formation encompasses dark grey limestones with subordinate grey shales. Biostratigrapically, the formation spans the *Paroistodus proteus* zone and ranges up into the basal *Prioniodus elegans* zone (Sturkell 1991).

The carbonate facies comprises extensively recrystallised fine grained nodules, surrounded by an often better preserved wackestone matrix (Fig. 15B). The basal decimetre contains glauconite grains which make up below 5% of the rock, but glauconite is otherwise absent in the formation. Up to six hardgrounds occur at regular intervals between -40.36 and -39.91. These are corrosional in character and have amplitudes of up to 4 cm (Fig. 15C).

4.2.3 Tøyen Shale Formation

The Tøyen Shale Formation is 6.3 m thick in the Brunflo #2 core and consists of dark grey shales with interbeds of trilobite wackestones (Fig. 15D). The base of the Tøyen Shale Formation is diachronous in the Jämtland area, beginning in the *Tetragraptus phyllograptoides* Zone in the Flåsjön area whereas the section in Kloxåsen starts in the *Phyllograptus densus* Zone (Jaanusson et al. 1982).

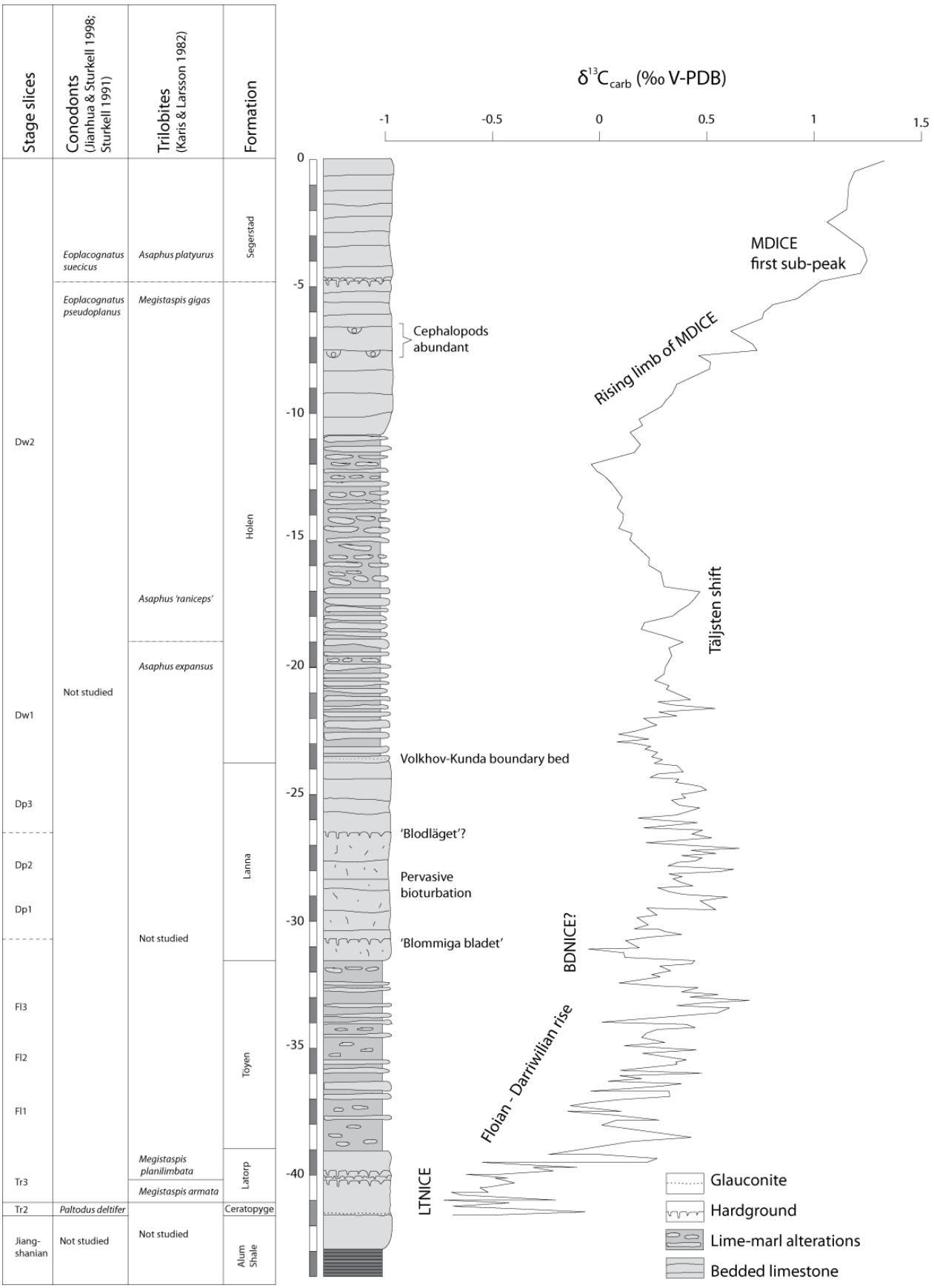

Fig. 14. Log of the Brunflo #2 core with carbon isotope curve, partly based on Wu et al. (in press).

Table 2A. Elemental composition of glauconite in the basal bed of the Ceratopyge Limestone.

Grain no.	Mg	Al	Si	K	O	Total
1	3.34	9.74	29.98	9.5	46.97	99.54
2	3.4	9.37	30.16	9.27	46.82	99.01
3	3.24	9.94	29.87	9.27	46.9	99.21
4	3.36	9.88	30.29	9.54	47.46	100.52
Mean	3.34	9.73	30.08	9.40	47.04	99.57

Table 2B. Elemental composition of glauconite in the upper bed of the Ceratopyge Limestone.

Grain no.	Mg	Al	Si	K	O	Total
1	3.27	10.19	30.33	9.09	47.63	100.52
2	3.23	9.79	28.64	8.91	45.28	95.85
3	3.56	9.32	29.55	9.13	46.17	97.74
4	3.07	11.28	29.37	8.98	47.35	100.04
Mean	3.28	10.15	29.47	9.03	46.61	98.54

The limestone beds of the formation are commonly less than 0.05m thick, but at -35.5m a 0.25 m thick bed can be observed. Above -34 m, the content of bioclasts increases both in the shale and in the limestone facies. This makes the shales turn a lighter shade of grey. Gradually, the shale content also decreases up to the base of the overlying Lanna Limestone.

4.2.4 Lanna Limestone

The 7.2 m thick Lanna Limestone comprises compact trilobite wackestones. It contains a diverse shelly fauna and may biostratigraphically be divided into the three biozones of *Megistaspis lata* (equivalent to *Megistaspis polyphemus*), *Megistaspis simon* and *Megistaspis limbata*, in ascending order (Karis 1998; Jaanusson et al. 1982).

The Lanna Limestone takes on a red colour but ubiquitous greenish *Thalassinoides* burrows contrasts strongly against the host rock. The formation is partly nodular owing to the presence of clay seams and marl beds.

Hardgrounds occur at two levels in the formation. The first level is a 7 cm thick interval with repeated hardgrounds (Fig. 15E) which can be found at ~30.6 m. This interval may possibly be an expression of the wide -spread hardground complex 'Blommiga bladet' (Lindström 1979). Another hardground is present at -28.58 cm. It is manifested as a sharp facies shift from limestone to shale, with up to 5 cm deep burrows or borings protruding down from the upper surface (Fig. 15F). This hardground may correlate with 'Blodläget' (Lindström 1979).

4.2.5 Holen Limestone

The Holen Limestone can be divided into two informal members on the basis of its expression in the Brunflo # 2 core; the lower one of these is characterised by rhythmic lime-marl alternations whereas the upper one is a compact, thick bedded limestone. Löfgren (1978) defined the lower one as the Flåsjö Limestone and the upper one as Järvsand Limestone. The lower part of the formation preserves a rich fauna belonging to the *Asaphus expansus* Biozone (Jaanusson et al. 1982).

The base of the Holen Limestone is marked by a limestone clast conglomerate over a weakly defined erosional surface in many parts of Jämtland (Karis 1998). Such an interval is not evident in the Brunflo core, but at ~-23.7 m, a 0.05 m thick glauconitic grainstone bed with a sharp, scoured base can be observed (Fig. 15G); a level which likely correlates with the conglomerate, and which would thus mark the base of the Holen Limestone. The glaucony in this bed is represented by light green, elongate grains. The base of the Holen limestone is also marked by the transition from *M. limbata* to *A. expansus* biozones, i. e. the Volkhov-Kunda transition in the Baltoscandian regional stages. This interval marks a pronounced sea level fall throughout Baltoscandia (Lindskog et al. 2014). This is concordant with the scoured base of the glauconitic bed discussed above, which indicates a significant sea level change.

The lower informal member, the rhythmites of the Flåsjö Limestone, can be subdivided into a lower part with medium thick limestone beds and an upper part with lenticular limestone nodules. The lower part comprises medium bedded, dark grey, wavy continuous bands of brachiopod and trilobite wackestone (Fig. 15H), interbedded with marly shales. This facies is overlain by discontinuous nodular limestones at -16.5 m, which show thicker marl interbeds. The marl beds gain a progressively darker colour higher up, peaking at -11.80 m. After this they become more shell rich and less dark.

The upper informal member, the Järvsand Limestone, is instead characterised by compact and thick dark grey limestone beds. Shale content is low. Just as in the Flåsjö limestone, the fauna is dominated by trilobites and brachiopods, but an interval at -7.80 to -6.40 m yield abundant endoceratid conches.

4.2.6 Segerstad Limestone

The Segerstad Limestone is not defined on lithological grounds; it is a topostratigraphical unit in which the base is defined by the appearance of the trilobite *Asaphus platyurus* (Jaanusson 1960). As such, it is hard to pinpoint the base of the Segerstad Limestone since no trilobite biostratigraphical work has been performed on the Brunflo core. Nonetheless, Larsson (1973) mentions several hardgrounds just above the base of the Segerstad Limestone. Three haematite impregnated hardgrounds of corrosional type occur at -4.90 m in the Brunflo core (Fig. 15I), and these may well correlate to

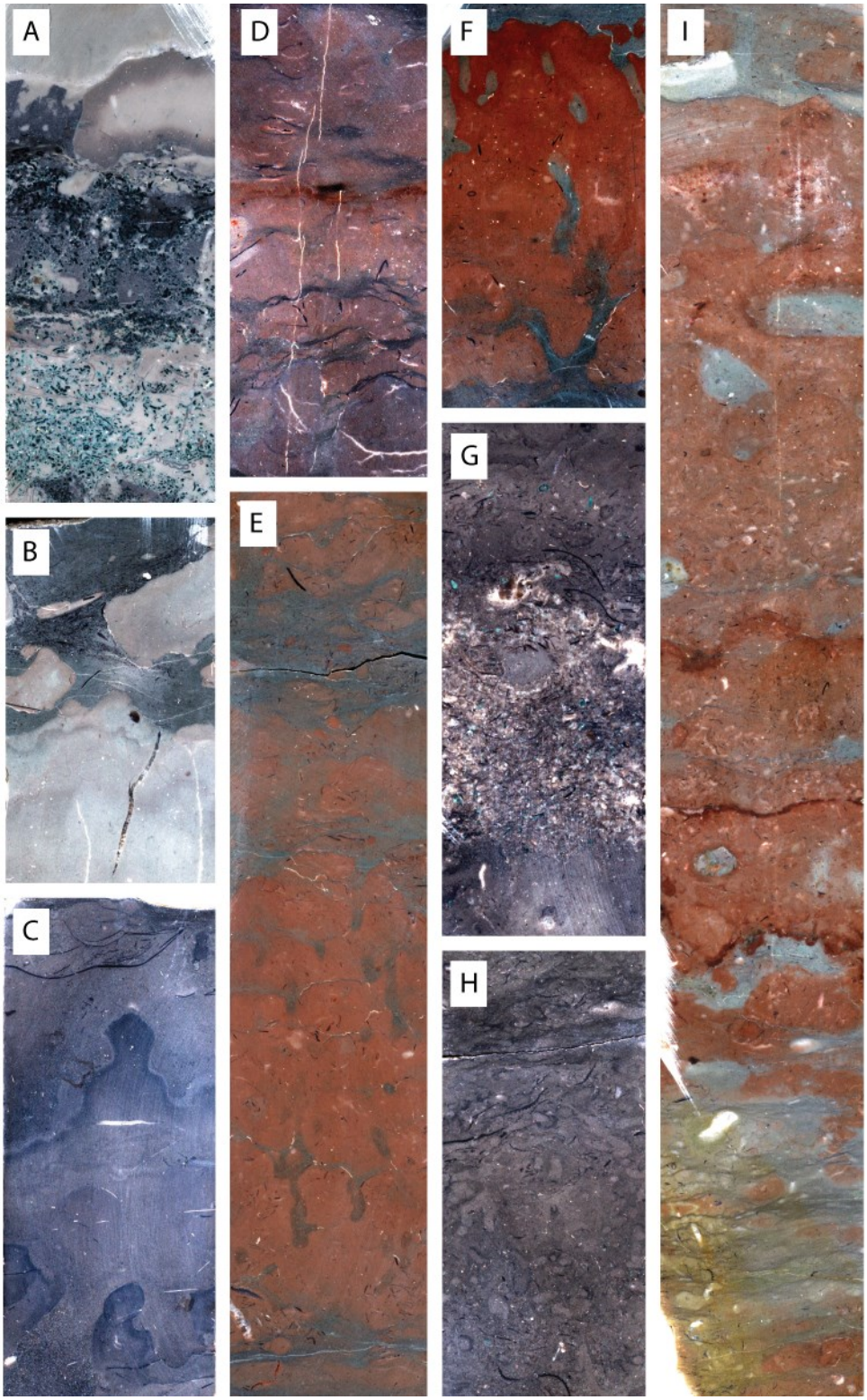

Fig. 15. Polished and scanned slabs from Brunflo #2 core, from Wu et al. (in press). Field of view is 3 cm wide. (A) The two beds of the glauconitic Ceratopyge Limestone. The glaucony of the upper bed is darker and have higher potassium content. Two pseudosparitic nodules in the upper part represent the lowermost Latorp Formation. (B) Recrystallized limestone clasts set in a dark grey wackestone matrix. (C) The middle part of the Latorp Limestone is characterized by corrosional hardgrounds, note the marked and irregular morphology of these two. (D) Typical lithology of the limestone beds of the Tøyen Formation. Possible escape trace can be seen in the upper left corner. (E) Hardground complex tentatively correlated with 'Blommiga bladet' (*sensu* Lindström 1979) in the lower part if the image. (F) Well defined hardground possibly corresponding to 'Blodläget' (Lindström 1979). (G) Glauconitic bed with sharp scoured base, interpreted as the Volkhov-Kunda boundary. (H) The lowermost part of the Holen Formation comprised thick bedded wackestone interbedded with marls. (I) Three haematite impregnated hardgrounds approximate the base of the topostratigraphical Segerstad Limestone in the core.

those described by Larsson (1973). They can thus serve to approximate the base of this unit. Lithologically, the Segerstad Limestone is, just as the upper part of the Holen Limestone, dominated by thick bedded trilobite wackestones. The rock is generally red, except where bioturbation has altered the rock green or grey. Minute pyrite crystals can be found dispersed throughout the unit.

5 $\delta^{13}C$-record

While the global record of the Upper Ordovician feature several well-studied high amplitude carbon isotope excursions, the Lower and Middle Ordovician is characterised by having smaller isotope shifts and a more subdued generalised curve (Bergström et al. 2009). The most prominent excursion in the Lower and Middle Ordovician is the mid-Darriwilian carbon isotope excursion (MIDICE; e.g. Meidla et al. 2004; Ainsaar et al. 2010; Schmitz et al. 2010), but lately, several smaller scale excursions have been described from Baltoscandia (Lehnert et al. 2014). Four of these are of interest of the present study, namely LTNICE (Late Tremadocian Negative Isotopic Carbon Excursion), BFICE (Basal Floian Isotopic Carbon Excursion, which marks the onset of the Floian-Darriwilian rise), BDNICE (Basal Dapingian Negative Isotopic Carbon Excursion) as well as the LDNICE (Lower Darriwilian Negative Isotopic Carbon Excursion). In Lehnert et al. (2014) , the LDNICE is present in the lower Darriwilian (lower Kunda) and precedes the MDICE, which shows peak values in upper Dw2 and basal Dw3 (Ainsaar et al. 2010).

5.1 Slemmestad

The $\delta^{13}C_{carb}$ data from Slemmestad (Fig. 10, Tables 3–4) show strongly fluctuating and surprisingly low $\delta^{13}C_{carb}$-values, and should thus be treated with caution. No clear trend can be seen in the dataset. When compared to the global $\delta^{13}C_{carb}$ curve by Bergström et al. (2009; which for this interval is based on data from Baltica by Kaljo et al. (2007)) the results presented here are about 2 ‰ lower, i.e. significantly shifted to the negative side. Similarly low and fluctuating results have been presented fot the Svartodden Member from another locality in the Oslo area (Guttormsen 2012). The poor data likely reflects diagenetic disturbances of carbon isotopes in the region. The Bjørkåsholmen Formation shows the most fluctuating values, which ranges between -0.8 and -12.3 ‰. Samples from recrystallised horizons and domains show the lowest values, so the fluctuations can at least be partly attributed to recrystallisation processes during early diagenesis.

Exposure with associated weathering and percolation of organic-rich humic fluids may shift isotopic signatures to more negative values (Saltzman & Thomas 2012). This is likely the case in the two uppermost samples in the Helskjer Member that show values around -6 ‰ and which were recovered from weathered rock just below the soil horizon. The other samples from Slemmestad were extracted from pristine rock that likely has not been altered by humic fluids. Alteration of the isotopic signature may in this case be derived from tectonic overburden during the subsequent Caledonian Orogeny. Conodont colour alteration palaeotermometry shows that temperatures reached 300 °C during the orogeny (Bergström 1980).

Table 3. $\delta^{13}C_{carb}$ data from the Bjørkåsholmen Formation.

Sample	Height (m)	$d^{13}C_{carb}$ (V-PDB)	Lithology
B1	0.01	-10.37	Recrystallized
B1b	0.02	-0.80	Wackestone nodule
B1c	0.05	-10.15	Recrystallized
B1d	0.06	-0.77	Wackestone nodule
B1e	0.15	-1.75	Black nodule
B2	0.25	-7.31	Recrystallized
B2b	0.30	-7.32	Recrystallized
B3	0.34	-1.42	Wackestone
B3b	0.38	-12.13	Recrystallized
B4	0.41	-12.28	Recrystallized
B5	0.46	-0.68	Wackestone
B6	0.52	-11.82	Recrystallized
B7	0.58	-0.45	Wackestone
B8	0.90	-0.89	Mudstone
B9	1.00	-8.09	Glauconite bed'
B10	1.15	-5.01	Glauconite bed'

The $\delta^{13}C_{org}$-curve from the Tøyen Shale Formation is more stable and is thus inferred to be more reliable. The data shows a generally decreasing trend throughout the Hagastrand Member, with some deviations (Fig. 9, Table 5). The first appearance of *Tetragraptus phyllograptoides* marks the base of the Floian, and this interval is slightly below the base of the Galgeberg member (*sensu* Owen et al. 1990). This coincides with a 3.5 ‰ positive excursion, after which a shift to increasing values is seen. An excursion peak followed by a rising trend fits with BFICE and the onset of the Floian-Darriwilian rise of Lehnert et al. (2014). Caution should be exercised however, as this would-be-excursion is represented by a single sample. A higher resolution would be preferable to confirm this excursion. Furthermore, $\delta^{13}C_{carb}$-values do not always correspond to similar trends in $\delta^{13}C_{org}$ as they are controlled by different factors (cf. Young et al. 2008).

The upper exposure shows a slightly increasing trend but no clear excursions. The uppermost sample show very high values but this sample was very rich in carbonate, and it is plausible that carbonate leaching was not sufficient during treatment in the lab of this particular marl sample.

Table 4. $\delta^{13}C_{carb}$ data from the Huk Formation

Member	Sample	Height above base of member	$\delta^{13}C_{carb}$ (V-PDB)
Hukodden	B44	0.02	-2.32
Hukodden	B45	0.10	-5.70
Hukodden	B46	0.18	-0.91
Hukodden	B47	0.27	-0.93
Hukodden	B48	0.34	-0.93
Hukodden	B49	0.40	-1.21
Hukodden	B50	0.51	-1.22
Hukodden	B51	0.66	-2.02
Hukodden	B52	0.75	-1.53
Hukodden	B53	0.85	-1.89
Hukodden	B54	0.95	-1.20
Hukodden	B55	1.09	-1.73
Hukodden	B56	1.23	-1.50
Hukodden	B57	1.34	-0.86
Hukodden	B58	1.47	-4.29
Hukodden	B59	1.58	-1.17
Hukodden	B60	1.67	-1.24
Lysaker	B61	0.05	-1.78
Lysaker	B62	0.12	-2.05
Lysaker	B63	0.26	-1.85
Lysaker	B64	0.36	-2.41
Lysaker	B65	0.52	-1.93
Lysaker	B66	0.63	-1.36
Lysaker	B67	0.78	-1.49
Lysaker	B68	0.90	-1.53
Lysaker	B69	1.00	-2.72
Lysaker	B70	1.07	-1.65
Lysaker	B71	1.15	-2.14
Lysaker	B72	1.25	-1.91
Lysaker	B73	1.37	-2.10
Lysaker	B74	1.51	-1.94
Lysaker	B75	1.68	-1.60
Lysaker	B76	1.83	-1.84
Lysaker	B77	1.94	-1.31
Lysaker	B78	2.03	-5.35
Lysaker	B79	2.16	-3.07
Lysaker	B80	2.23	-1.79
Lysaker	B81	2.41	-1.38
Lysaker	B82	2.59	-1.86
Lysaker	B83	2.68	-2.35
Lysaker	B84	2.79	-1.49
Lysaker	B85	2.95	-2.11
Lysaker	B86	3.04	-2.99
Lysaker	B87	3.16	-1.99
Cont.			
Lysaker	B88	3.25	-1.96
Lysaker	B89	3.37	-1.45
Lysaker	B90	3.45	-1.74
Lysaker	B91	3.56	-1.61
Lysaker	B92	3.70	-1.32
Lysaker	B93	3.84	-1.18
Lysaker	B94	3.98	-1.89
Lysaker	B95	4.03	-1.26
Lysaker	B96	4.14	-0.90
Lysaker	B97	4.23	-2.10
Lysaker	B98	4.28	-2.49
Lysaker	B99	4.35	-1.37
Lysaker	B100	4.41	-3.67
Svartodden	B100b	0.02	-1.19
Svartodden	B101	0.11	-1.86
Svartodden	B102	0.24	-1.08
Svartodden	B103	0.36	-0.72
Svartodden	B104	0.54	-3.56
Svartodden	B105	0.60	-2.69
Svartodden	B106	0.72	-4.23
Svartodden	B107	0.79	-0.85
Svartodden	B108	0.89	-4.11
Svartodden	B109	1.05	-0.52
Svartodden	B110	1.19	-0.85
Svartodden	B111	1.24	-1.12
Svartodden	B112	1.28	-3.03
Svartodden	B113	1.39	-4.80
Svartodden	B114	1.48	-1.82
Svartodden	B115	1.61	-0.89
Svartodden	B116	1.68	-0.71
Svartodden	B117	1.81	-1.97
Svartodden	B118	1.89	-1.78
Svartodden	B119	1.97	-1.16
Svartodden	B120	2.09	-1.41
Svartodden	B121	2.19	-1.41
Svartodden	B123	2.37	-1.64
Svartodden	B122	2.40	-2.26
Helskjer	B124	0.05	-2.97
Helskjer	B125	0.12	-2.41
Helskjer	B126	0.21	-2.03
Helskjer	B127	0.25	-2.01
Helskjer	B128	0.45	-2.88
Helskjer	B129	0.59	-1.97
Helskjer	B130	0.68	-1.70
Helskjer	B131	0.80	-6.33
Helskjer	B132	0.96	-5.74

Table 5A. $\delta^{13}C_{org}$ data from the lower exposure, Tøyen Shale Formation

Member	Sample	Height above base of member	$\delta^{13}C_{org}$ (V-PDB)
Hagastrand	B11	0.13	-26.83
Hagastrand	B12	0.63	-26.84
Hagastrand	B13	1.14	-27.59
Hagastrand	B14	1.74	-27.69
Hagastrand	B15	2.17	-27.08
Hagastrand	B16	2.67	-27.13
Hagastrand	B17	3.30	-27.97
Hagastrand	B17(II)	3.30	-28.09
Hagastrand	B18	3.70	-27.45
Hagastrand	B19	4.20	-26.92
Hagastrand	B20	4.78	-28.29
Hagastrand	B20(II)	4.78	-28.30
Hagastrand	B21	5.21	-26.90
Hagastrand	B22	5.67	-26.77
Hagastrand	B23	6.13	-29.91
Hagastrand	B24	6.69	-27.83
Hagastrand	B25	7.22	-26.96
Hagastrand	B26	7.65	-28.95
Hagastrand	B27	8.32	-29.20
Hagastrand	B28	8.99	-29.14
Hagastrand	B29	9.65	-29.35
Hagastrand	B30	10.06	-28.00
Hagastrand	B31	10.56	-29.39
Hagastrand	B32	11.16	-25.75
Hagastrand	B33	11.50	-29.63
Hagastrand	B34	12.12	-29.05
Hagastrand	B35	12.84	-27.76

Table 5B. $\delta^{13}C_{org}$ data from the upper exposure, Tøyen Shale Formation

Member	Sample	Height below base of Huk Fm.	$\delta^{13}C_{org}$ (V-PDB)
Galgeberg	B36	-3.44	-30.13
Galgeberg	B37	-2.87	-29.05
Galgeberg	B38	-2.48	-29.81
Galgeberg	B39	-1.9	-28.98
Galgeberg	B40	-1.35	-29.01
Slemmestad	B41	-0.86	-28.22
Slemmestad	B42	-0.34	-28.97
Slemmestad	B43	-0.02	-25.44

5.2 Brunflo

As opposed to the carbon isotope studies from Slemmestad, the Brunflo data shows reliable values throughout the studied interval. The Brunflo core #2 shows a general increasing trend in $\delta^{13}C_{carb}$, starting with the values of approximately -0.5 ‰ of the Latorp Formation, and ending at over +1.3 ‰ in the Segerstad Limestone, with a number of smaller fluctuations and subtrends in between (Fig. 14). The Latorp Formation records a dip which likely corresponds to the LTNICE of Lehnert et al. (2014). The curve rises and shifts to positive values at the transition to the overlying Tøyen Shale Formation, continues to rise and culminates in a peak near the top of the formation, reflecting the lower part of the Floian-Darriwilian rise (Lehnert et al. 2014). Values drop to below zero at the transition between the Tøyen and Lanna formations, possibly representing the Basal Dapingian excursion of Lehnert et al. (2014), an interesting interval as it is just below the regionally important hardground complex 'Blommiga bladet'. The isotope data from the Lanna Limestone show a bulge, starting at low values, with higher values in the middle that drop again near in the transition to the Holen Formation. This interval marks the transition between the Volkhov and Kunda regional stages. Meidla et al. (2004) also documented a negative excursion at this interval in the Gullhögen quarry in Västergötland, just a metre below the conspicuous 'Täljsten' interval.

Values in the lower member of the Holen Formation vary between 0 and 0.5 ‰, showing a series of fast shifts beween -19 and -17 m that may have correlational importance, as the 'Täljsten' interval in Meidla et al. (2004) is also marked by a series of fast shifts. A fast shift exceeding 0.6 ‰ can also be seen in the data from Tingskullen of Wu et al. (submitted) at the transition from *Lenodus variabilis* and the *Yangtzeplacognathus crassus* zones, which is time equivalent to the 'Täljsten' (Mellgren & Eriksson 2009).

A distinct negative excursion with a magnitude of 0.5 ‰ is present at the transition to the upper member of the Holen Limestone where it marks the onset of the MDICE. The excursion has previously been interpreted as the LDNICE (Wu et al. in press) but the level is likely too high up in the stratigraphy as the LDNICE was originally defined by Lehnert et al. (2014) to be in the basal Kunda and the 'Täljsten' interval. The LDNICE as originally defined by Lehnert et al. (2014) is likely best represented by the 'Täljsten' shift metioned above.

The upper member of the Holen and the Segerstad limestones show a strong and steady increase in $\delta^{13}C_{carb}$-values, going from 0 to 1.3 ‰. The stratigraphic position as well as the magnitude of the excursion corresponds to the rinsing limb of MDICE (Meidla et al. 2004; Ainsaar et al. 2010). This excursion is characterised by three subpeaks, and the first of these is represented in the uppermost part of the Holen Formation. The second and highest peak of MDICE is not preserved in the core interval.

6 Comments to lithology

6.1 Pseudomorphs, recrystallisation and possible implications

Major recrystallisation characterises the Bjørkåsholmen Formation and the Latorp Limestone in the Brunflo core section and presumed pseudomorphs of evaporitic minerals are also found in the Bjørkåsholmen Formation and the Hagastrand Member in Oslo. The most conspicuous of the presumed evaporite pseudomorphs are those found in 'the main limestone bed' of the Bjørkåsholmen Formation in Oslo. Here, the spatial relationship between the presumed evaporite pseudomorphs and limestone nodules indicates that the evaporite crystals grew within the sediments, thereby displacing the nodules (esp. in Fig. 8B). Demicco & Hardie (1994) writes that sediment displacive growth of evaporites unequivocally means that evaporitic conditions has occurred, but it is uncertain whether these were met closely after deposition or later during diagenesis by saturated deep brines. According to Kendall & Harwood (1996) supersaturated brines are only likely to be formed at the brine-air interface. This would mean that the crystals formed penecontemporaneously to deposition and that depositional depth cannot be more than a few metres deep. This is because deep bodies of brine almost always are stratified, and concentrated surface brines do not descend to the basin floor. Furthermore, in modern environments, sulphates form in marginal marine settings and become more dominated by halite shorewards (Kendall & Harwood 1996). We do not see signs of halite – no cubic crystals – indicating that the Bjørkåsholmen Formation was likely deposited in a shallow environment.

The crystal mushes indicate that gypsum was abundant. This type of displacive crystal growth normally forms in association with algal mats or fine grained sediment (Kendall & Harwood 1996). The latter is more likely as neither filaments, fenestrae nor other indications (Tucker 2001) of algal mats are found. These crystals are set in a matrix which shows a transition of pseudospar to microspar and micrite. This phenomenon is briefly discussed in Scholle & Ulmer-Scholle (2003). They write that the mecahanism behind is not fully understood, but that such recrystallisation is often associated with early meteoric exposure and tectonic stresses or large scale, syndepositional, glacioeustatic sea level fluctuations.

While Egenhoff et al. (2010) mentioned heavy recrystallisation of the Norwegian successions, they did not discuss why this is the case. According to them, crystal sizes reflect original grain size, i.e. the fine grained recrystallised rock derive from mud- or wackestones whereas the coarse grained ones reflect packstones. By this way of reasoning, they recognise fourteen deepening upwards cycles in the strata, based on the perceived fining upwards trend in the carbonates. In my opinion however, recrystallisation of the for-

mation is so severe that such conclusions cannot be drawn. This is evident from both texture and low $\delta^{18}O$-values (cf. Wu & Wu 1996). Crystal sizes of recrystallised material depend not only on primary clast size but also on mineralogy; abundant unstable primary aragonite allows for a high degree of secondary precipitates (cf. Lasemi & Sandberg 1984; Munnecke 1997).

The Latorp Limestone also shows recrystallisation structures similar to the ones seen in the Bjørkåsholmen Formation, and may indicate that evaporitic and restricted conditions were more widespread in the Early Ordovician of Baltoscandia than previously thought. If so, why is this only at this level and not higher up? After all, climate must have been warmer as the continent was approaching the equator (Cocks & Torsvik 2005). According to Nielsen & Schovsbo (2013) the basin was silled, and a sea level drop could potentially produce lagoonal evaporitic conditions. Furthermore, the Early Ordovician represents a very warm period and is characterised by greenhouse conditions. However, sea surface temperature gradually cooled and reached modern equatorial sea surface temperatures during the Middle Ordovician, reflected by a drop of ~10°C from the middle Tremadocian to the Darriwilian (Trotter et al. 2008). Global climate change with major cooling of the Earth's oceans may thus be the driving factor behind the absence of evaporitic facies higher up in the Baltoscandian Ordovician successions.

6.2 Glaucony

Glauconite is, in the strict sense, a green, potassium and iron rich ferric micaceous mineral. It forms in marine sediments at intervals of slow deposition and often occurs in a granular habit (e.g. Hugget 2005). As Odin & Matter (1981) noted however, the term 'glauconite' is commonly both used for green grains in general as well as the facies in which it occurs. To avoid confusion, they proposed that the term 'glauconitic minerals' be used for the clay minerals that characterise the glaucony facies, i.e. a clay mineral family with a pronounced variation in potassium content, the end-members of which being a K-poor glauconitic smectite and a K-rich glauconitic mica. They also proposed the term 'glaucony' be used for the blue-green marine facies characterised by these green glauconitic minerals (see also Odin 1988).

Small pores of various substrates, ranging from skeletal debris to lithic grains to faecal pellets, provide favourable microenvironments for glauconitisation. These semi-confined conditions provide a chemistry that differs from both that of the sea water and the sediment pore-water as ion interchange with the surroundings does occur, but at a restricted rate (Odin & Matter 1981; Odin & Fullagar 1988). As iron is not mobile during oxidising conditions, and as iron tends to form pyrite in truly reducing milieus, glaucony is inferred to form in sub-oxic, slightly reducing environments during shallow burial (Kelly & Webb 1999). Sea water contains only traces of Al, Si and Fe and the chemical constituents of the glauconitic minerals may be supplied from the substrate grain as it dissolves (Clauer et al. 1992).

According to Odin & Matter (1981), the first mineral to form is a K-poor glauconitic smectite and as time progresses more and more smectite is formed. At the same time, the crystals that have already formed undergo a maturation process in which they gradually incorporate more K and become less expandable. In this maturation process the glauconitic smectite recrystallises into glauconitic mica and the original substrate grain tends to dissolve completely. K2O-content of glaucony in the nascent stage is between 2–4 wt % but rises and exceeds 8 wt % in the highly evolved stage (Odin & Fullagar 1988).

The mineralogy of glauconitic minerals is preferably studied using X-ray diffraction (XRD), as this kind of study allows for distinction between mica and smectite (Odin & Matter 1981). On the other hand, most of the physical properties, including e.g. XRD-patterns, density and paramagnetism of glaucony, can be correlated with the potassium-content (Odin & Fullagar 1988). An XRD-device has not been available to the present study, but energy-dispersive X-ray spectroscopy (EDX) was employed instead. While this method cannot differentiate between clay mineral lattices, it allows measurement of potassium content.

The potassium content of the glauconitic minerals of Bjørkåsholmen formation is on average 7.43% and can thus be considered to be of evolved type, a product of a maturisation process which may take over 105 years (Odin & Fullagar 1988). On the other hand, these minerals have likely been diagenetically altered (Bjørlykke 1974) and the results should thus be treated with caution. The data from the Ceratopyge Limestone are more reliable and show that the upper bed is more evolved than the lower bed, indicating a longer time of slow-deposition when this bed formed. Both beds can be considered as highly evolved, indicating a period of slow-deposition approaching 106 years for each of these beds (Odin & Fullagar 1988).

6.3 Limestone-marl alternations

The Lysaker Formation is best described as a limestone-marl alternation *sensu* Munnecke & Samtleben (1996). Here, the term 'marl' is not used in a strict sense, i.e. as a specific lime/clay ratio, but as a designation for the part of the rock that weathers out more easily. Limestone-marl alternations are thought to form in the shallow, early diagenetic realm due to dissolution of aragonite and subsequent precipitation as calcite. At a certain depth ('Aragonite Solution Zone' or ASZ), the pore water chemistry renders aragonite unstable and it is dissolved. This zone where dissolution occurs will come to form the marly horizons. The calcium carbonate migrates upwards where it reprecipitates as calcite, leading to what will become limestone layers (Munnecke & Samtleben 1996). On the other hand, aragonite dissolution may also occur at the sediment-water interface (Palmer & Wilson 2004). In this case,

aragonite is dissolved but does not reprecipitate as cement; instead the ions go into solution in the sea water. Nonetheless, in the model of Munnecke & Samtleben (1996), the lime-marl alternations are not formed due to inhomogenities in the precursor sediment but because to the presence of unstable aragonite. These alternations can thus not be used to infer climatic changes due to for instance Milankovitch fluctuations (Westphal 2006).

Preliminary palynological studies of various rhythmites of the Oslo Region, including the Lysaker Member, have been presented by Amberg et al. (2013). These show that the palynomorph assemblages of limestones and mudstones do not differ significantly. Furthermore, findings by Egger et al. (2013), who studied the Skogerholmen Formation of the Upper Ordovician in the Oslo Region, show that ratios of diagenetically insoluble elements (in this case Ti and Al) are essentially the same in both lithologies. This would not have been the case if the rhytmites were a primary feature and with significant differences in clay mineralogy composition at the time of deposition of lime and marl layers. Together, these two studies lend strong support to the hypothesis that the limestone-marl alternations derive from diagenetical processes and that these sediments were originally more or less homogenous.

The ratio of the marl and limestone thicknesses of marls and limestones depends on which calcium carbonate polymorph dominated the precursor sediment; a high content of aragonite would give rise to thicker limestone beds (Munnecke et al. 2001). The Lysaker Member does not only show rhythmic beds, it also shows cyclicity at a larger scale, with limestone beds being thicker and more prominent at certain levels. If the model of Munnecke & Samtleben (1996) is correct, this suggests that more aragonite as compared to calcite was precipitated at the time these levels became deposited. Which polymorph to be precipitated depends both on the marine Mg:Ca ratio as well as the temperature of ambient waters, with aragonite formation being favoured at high Mg:Ca ratios and high temperatures (Balthasar & Cusack 2015). The larger scale cyclicity that can be observed in the Lysaker Member may thus be a function of climate fluctuations.

7 Chemostratigraphy and environmental implications

Variations in $\delta^{13}C$ of the world's oceans through time have foremost been used for correlation. However, the $\delta^{13}C$ is mainly dependent on the distribution between organic carbon and carbonate rocks, and is thus directly linked to the global carbon cycle and the geobiosphere development (Saltzman & Thomas 2012).

Numerous factors influence the $\delta^{13}C$-development however, and the connections are not always clear-cut. Volcanism, the proportion of carbonate relative to silicate weathering and the composition of terrestrial vegetation are a few of the factors that influence the carbon isotope development (Kump & Arthur 1999). Numerous episodes of extinctions or biotic turnover have also been linked to carbon isotope excursions (Salzman & Thomas 2012).

The Ordovician Period records an unparalleled diversification among marine invertebrates. This evolutionary event has been coined 'The Great Ordovician Biodiversification' or GOBE (Webby et al. 2004), and its importance is on a par with the 'Cambrian explosion'. Whereas the latter generated a wide disparity and larger number of taxonomically higher ranking taxa, it was the former that provides the sheer biomass and any substantial biodiversity at genus and species level (Harper 2006). Tiering complexity increased and a number of new niches were also occupied, which for instance can be seen in the coeval increase of intensity and diversity of carbonate substrate bioerosion ('Ordovician Bioerosion Revolution' of Wilson & Palmer 2001, 2006).

Increased tiering and the occupation of new niches associated with the onset of GOBE likely led to a sheer increase in total biomass and, with that, increased burial of organic material. Organic material is enriched in light ^{12}C as compared to ^{13}C. Large scale burial of organic matter thus leads to that the oceans become depleted in the lighter isotope, giving a long term increasing trend in the $\delta^{13}C$-record (Knauth & Kennedy 2009). It has also been suggested that the increase in carbon burial rate lead to climatic cooling, which further stimulated the development of the GOBE (Trotter et al. 2008, Zhang et al. 2010). The Floian marks the start of a long-term rise in the carbon isotope record, the Floian-Darriwilian rise (Lehnert et al. 2014), a development which eventually culminates in the MDICE. Does this timing fit with the timing of the GOBE?

To begin with, the biodiversification event was by no means a continuous steady increase in species and genera, but followed a stepwise pattern, varying for different taxonomical groups (Webby et al. 2004; Harper 2006). To some extent, these biodiversity peaks reflect sea level; graptolites peak at high sea levels whereas the opposite is seen with ostracodes and brachiopods. This gives a general trend where high sea levels correspond with low biodiversity and vice versa (Hammer 2003; but this may well just be a taphonomical effect, as the shallow water sediments deposited during highstand are preferentially eroded away, and thus also the fossils). On Baltica, the GOBE is expressed as four distinct peaks in diversity: one at the beginning of the Floian Stage, one in the upper Dapingian/lower Darriwilian (Langevoja regional substage), one in the late Sandbian and finally one in the Katian. Conversely, the Dw2 and Dw3 record a prominent dip in diversity (Hammer 2003).

The onset of the Floian-Darriwilian rise thus matches with the onset of the GOBE, whereas the MDICE corresponds to a diversity dip. Interpreting environmental signals from the $\delta^{13}C$-record is by no

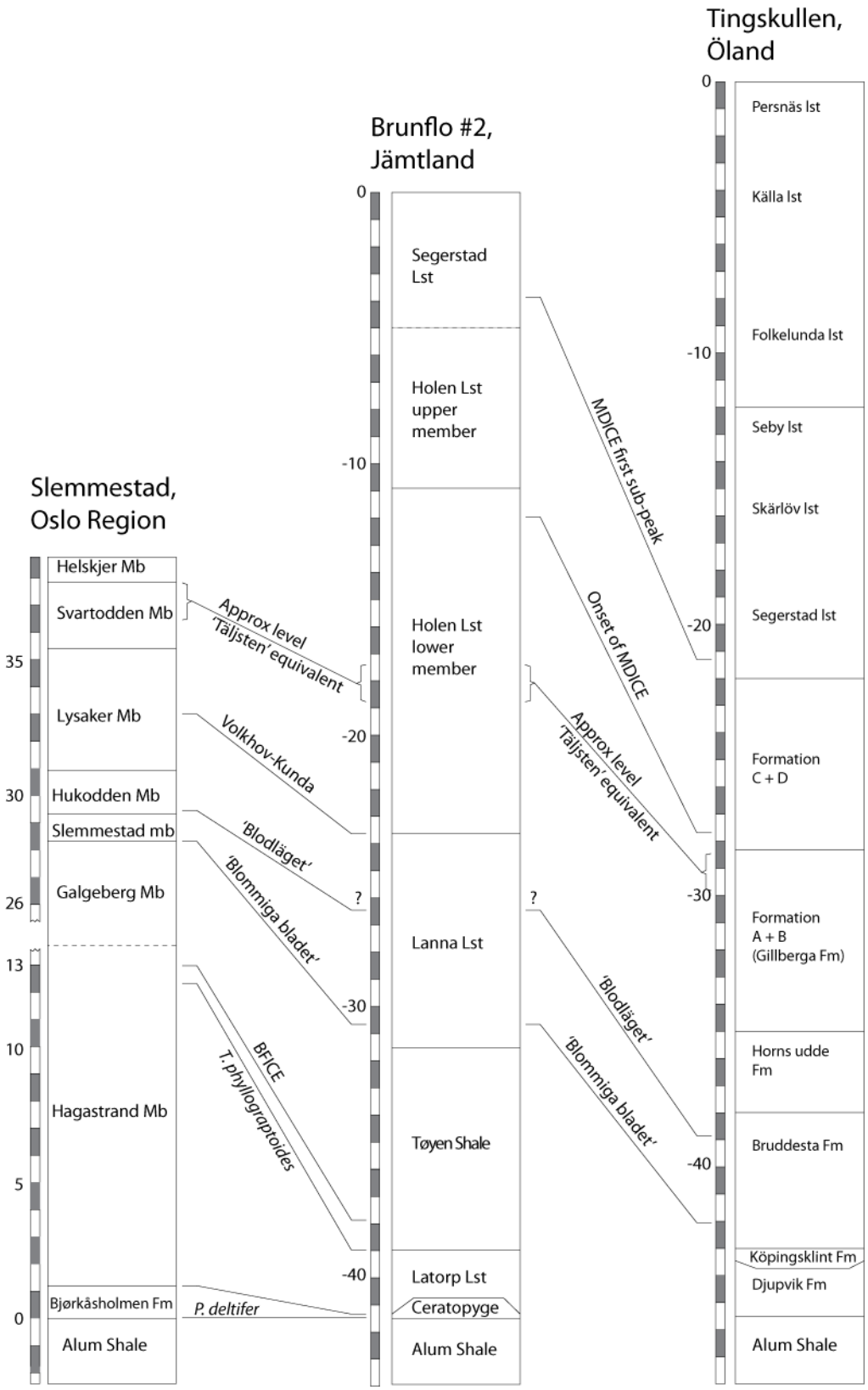

Fig. 16. Correlation of Lower–Middle Ordovician strata across western Baltoscandia, based on carbon isotope stratigraphy, widespread hardground complexes and biostratigraphy. See text for detailed discussion.

means straightforward, and a simple correlation between diversity and carbon isotope trends does not exist.

8 Correlation and depositional history

To correlate the sections in Oslo and Jämtland, an integrated approach is adopted here by combining biostratigraphic data with carbon isotope trends and microfacies analysis, with the main results presented in Figure 16. The sections in Slemmestad and Brunflo both represent relatively deep marine facies on the western margin of Baltica, although Slemmestad had a generally deeper setting with a higher siliciclastic influx. The Norwegian successions are considerably more expanded, especially during Tremadocian and Floian times.

As no analogues of the vast, epicratonic seas that characterised the Early Palaeozoic exist today, sea level interpretation and application of sequence stratigraphy for these successions is problematical. Nonetheless, various techniques may be used to deduce palaeo-sea levels, including sedimentological evidence, physical proxies (such as regional relief), ecology and biological assemblages as well as geochemical data of oxygen isotopes (Munnecke et al. 2010). Studying the Upper Ordovician successions of western Estonia, Harris et al. (2004) used the depositional texture in the classification scheme of Dunham (1962) as a basis for a model to interpret epicratonic seas. In their model, facies belts shift laterally from shelf to basin with grain supported facies being deposited in the shallow shelf, mixed facies in the middle shelf, mud-supported facies in the deep shelf and slope and finally black shale facies in the basin (Fig. 17). While this makes sense intuitionally, one must bear in mind that it is a simplified model and that carbonate sediments are biologically formed sediments – i.e. they are affected not only by sea level but also for instance by climatic factors. Nonetheless, the simplicity of the model makes it useful for interpretations.

Ordovician sea level curves have been reconstructed for several continents, e.g. Laurentia (Ross & Ross 1992, 1995), Sibiria (Kanygin et al. 2010) and the Yangtze Platform (Su 2007). Long ranging sea level curves for the Ordovician of Baltoscandia include those by Nielsen (2004) and Dronov et al. (2011). Nielsen (2004) focussed on the Scandinavian, distal parts of the basin whereas Dronov et al. (2011) based their curve on the proximal parts in the shallow-water settings of Estonia.

These roughly correspond to one another in the Tremadocian and Floian but differ considerably in the Dapingian and Darriwilian; Nielsen (2004) inferred a lowstand at the same time as Dronov (2011) perceived a highstand. This contradiction is partly based on the fact that their curves are based on the distal and proximal parts of the platform respectively but also because they used different approaches to reconstruct sea level. Dronov et al. (2011) base their assessments on two assumptions that major regional unconformities represent forced regressions and that the expansion over a wider area of deep water facies, such as marine red beds, reflect transgressions. However, it may be argued that, as regional unconformities expressed as hardgrounds represent highly condensed strata (Flügel 2010), sea level falls cannot be deduced from these.

8.1 Tremadocian 2

The interval of interest for the present study starts in the Tremadocian 2 time slice with the deposition of the Bjørkåsholmen Formation and Ceratopyge Limestone. Both belong to the *P. deltifer* Zone (Sturkell 1991; Erdtmann & Paalits 1994). This zone has not been documented from Tingskullen, and the time interval represented by the Bjørkåsholmen Formation and the Ceratopyge Limestone may simply be gone due to erosion in association with the karstic level at 46 m in the Tingskullen core.

The sudden transition from the black, anoxic Alum Shale to the possibly evaporitic limestones of the Bjørkåsholmen Formation suggests a significant sea level drop (Fjelldal 1966, Erdtmann & Paalits 1994, Nielsen 2004). The formation has been interpreted as representing a lowstand systems tract (Dronov & Holmer 1999) or as a falling stage systems tract with a

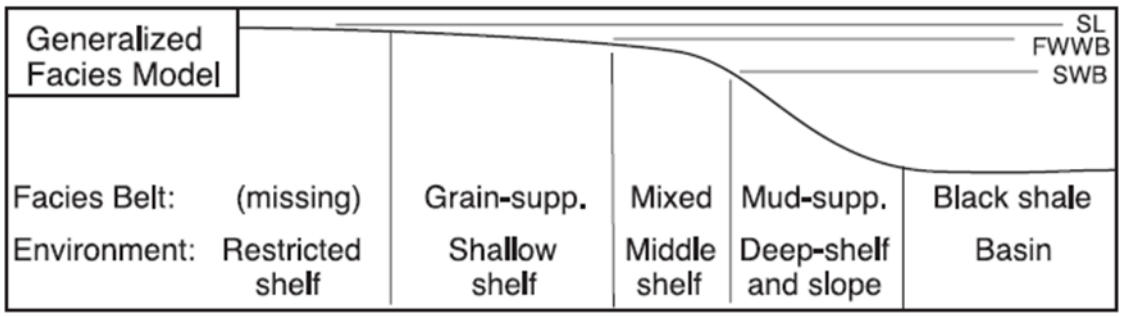

Fig. 17. Facies model originally constructed for the Upper Ordovician of Western Estonia (Harris et al. 2004), but a similar large scale morphology and sedimentation pattern likely prevailed in western Baltoscandia during the Lower and Middle Ordovician times. Key to abbreviations: SL = sea level, FWWB = fair-weather wave-base and SWB = storm wave-base.

superimposed lowstand systems tract (Egenhoff et al. 2010). The Bjørkåsholmen Formation is 1.2 m thick whereas the Ceratopyge Limestone is only 0.05 m in thickness. While the Bjørkåsholmen rests conformably atop the Alum Shale, a hiatus that spans part of the Cambrian Jiangshanian stage to the basal Tremadocian underlies the Ceratopyge Limestone in Brunflo. This suggests a sea level fall that exposed the Cambrian sediments to erosion in Brunflo but that the magnitude of the fall was not sufficient to expose the Slemmestad strata.

Egenhoff et al. (2010) proposed that the regression was an isostatic event due to uplift in association with an early stage of the Caledonian Orogeny. Erdtmann & Paalits (1994) on the other hand regarded it as eustatic, the Ceratopyge Regressive Event (CRE). It coincides with the transition between the Sauk III and Tippecanoe I megacycles in North America, and Nicoll et al. (1992) considered it identical with the Kelly Creek Eustatic Event recognised in the Georgina and Amadeus basins of Australia. Erdtmann & Paalits (1994) discussed a possible glacial influence, but only controversially discussed tillites have been found from this time. Furthermore, this period was characterised by greenhouse conditions (Trotter et al. 2008) rendering glacial episodes unlikely. What is clear is that the regression coincides with a major faunal turnovers and extinctions in for instance conodonts, graptolites and trilobites in many parts of the world (Erdtmann & Paalits 1994, Albanesi & Bergström 2004).

The CRE was followed by a long term transgression (Nielsen 2004). The glaucony of the Ceratopyge Limestone and Bjørkåsholmen Formation may thus have formed during the transgression following the sea level fall. A model outlined by Amorosi (1995) predicts that the abundance as well as the maturity of glaucony increases through the upper transgressive systems tract, reaching a peak at the condensed section, and is followed by a gradual decrease in the highstand systems tract. This model fits with the observation of increasing maturity of glaucony in the Ceratopyge Limestone as well as the findings of a few scattered glauconite grains in the basal parts of the overlying Latorp Limestone. The initial precipitation of glauconitic smectite is estimated to occur in a time-span of 1– 10 kyr whereas highly evolved glauconitic mica takes 100–1000 kyr to form (Odin & Matter 1981). During this interval, the evolving glaucony must be kept at slightly reducing conditions and not be buried too deep. The presence of highly evolved glaucony thus speaks for a significant break in marine sedimentation (Odin & Matter 1981; Amorosi 1995, 1997; Kelly & Webb 1999). These conditions are more likely to occur during transgressions, when the sedimentation zone moves landwards (Odin & Matter 1981).

8.2 Tremadocian 3 and Floian

The biostratigraphic control on the Hagastrand Member (basal Tøyen Shale Formation in the Oslo Region) is poor, but it is deemed to be coeval with strata belonging to the *Megistaspis (Paramegistaspis) planilimbata* Zone (Hoel 1999a). This correlates with the upper part of the Latorp Limestone where this Biozone had been documented (Karis & Larsson 1982).

Sequence stratigraphic models are admittedly difficult to apply to deep water facies. Nonetheless, Egenhoff & Maletz (2007) introduced a way to work with sequence stratigraphy also in monotonous shale successions based on taxonomic varations among the graptolites. They found that endemic forms dominate most of the sedimentary interval, but that pandemic deep water taxa form mass-occurences at certain intervals. They hypothesised that these intervals represented maximum flooding surfaces. And indeed, Erdtmann (1965) also mentions mass occurrences of for instance *Clonograptus* and multiramous dichograptids at several levels in the Tøyen outcrop in Oslo, but only one of these were specified. This level is dominated by *Clonograptus galgebergi* and *Clonograptus norvegicus* and occurs at 3.55-3.68 in the Tøyen outcrop. It is equal to 'the 'good bed' of the *H. copiosus* fauna' (Lindholm 1991) and may correlate to a black shale bed at 7.1 m above the base at Slemmestad, thus likely representing a maximum flooding surface.

The base of the Tøyen Shale Formation in Jämtland is diachronous, and ranges between *Tetragraptus phyllograptoides* and *Phyllograptus densus* biozones (Jaanusson et al. 1982), the first of which is found in the uppermost part of the Hagastrand Member in Oslo and the latter which is found in the middle part of the Galgeberg Member (Erdtmann 1965). The 2.5 m thick Latorp Limestone thus correlates with at least the basal 11 m of the Hagastrand Member, making the Latorp Limestone extremely condensed. Recrystallisation and pseudomorphs are evident both in Slemmestad and in Brunflo in this interval.

The base of the Floian is marked by carbon isotope excursions in the Slemmestad and Brunflo sections; these are inferred to correspond to the BFICE of Lehnert et al. (2014). The facies transitions from grey shale with silt interbeds to black, anoxic shales in Oslo and the corresponding transition from compact limestone to lime-marl interbeds suggest a continued transgression at this time.

The Floian strata in Oslo is more expanded in Oslo than in Jämtland; the Tøyen Shale Formation is approximately 10 m thick in Jämtland, while the coeval Galgeberg and Slemmestad members is estimated to comprise more than 15 m of strata.

8.3 Dapingian

'Blommiga bladet' ('Flowery sheet') and 'Blodläget' ('Bloody layer') are extensive hardground complexes that can be followed over large parts of Scandinavia, from Öland in the SE to Dalarna in the NW, to the Baltic area in the east, serving as important marker horizons across the continent (Lindström 1979). The lowermost of these, 'Blommiga bladet', is

characterised partly by abundant amphora-like borings but foremost by its strong colours, ranging from yellow and red to green (Lindström 1979; Ekdale & Bromley 2001). Biostratigraphically, 'Blommiga bladet' formed at the base of *Baltoniodus triangularis* zone, which is the index fossil that marks the base of the Dapingian Stage (Bergström & Löfgren 2008). The exact location of this base has not been pinpointed in the Oslo region as the deep water facies of the Tøyen Shale Formation yield no conodonts (Bergström & Löfgren 2008), and the hardground complex is not developed in the same way in these shaly facies. Nonetheless, the location can be approximated using other biostratigraphic data. The transition from *Isograptus lunatus* to *Isograptus victoriae* biozones is at, or close to, the base of the *B. triangularis* zone (Bergström et al. 2009; Pärnaste et al. 2013). While *I. victoriae* has not been documented from the Tøyen Shale Formation, *I. lunatus* has been reported from a level approximately 3 m below the top of the formation (Erdtmann 1965). The base of the succeeding Huk Formation is within the *Baltoniodus navis* zone, i.e. its deposition took place well within the Dapingian Stage. The base of the Dapingian and the level of 'Blommiga bladet' must thus be within the uppermost 3 m of the Tøyen Shale Formation. This interval contains a multicoloured horizon at 1.3 m below the base of the Huk Formation interpreted as a maximum flooding surface. This level probably corresponds to 'Blommiga bladet', but developed in a deeper facies. It is overlain by the grey shales of the informal Slemmestad Member.

'Blommiga bladet' is not unequivocally expressed in the Brunflo core either, but it is tentatively recognised as the hardground complex found at -30.6 m, not even a metre above the base of the Lanna Limestone. The basis for correlation of these two beds is thus not very strong. The shift in facies from black shales to grey in Oslo and the reappearance of compact limestone (Lanna Limestone) in Brunflo suggest that the transgression that started in the late Tremadocian had culminated and turned into a regression. 'Blommiga bladet' is clearly expressed at -41.95 m in the Tingskullen core of Öland.

The other hardground level of interest is 'Blodläget'. This has been identified with a high degree of confidence at 0.17 m above the base of the Huk Formation in Slemmestad, coinciding with the base of *Megistaspis simon* Zone (Nielsen 1995). A pronounced hardground at -28.58 m in the middle Lanna Limestone may correspond to this level, as *M. simon* is found in the middle part of this formation (Karis 1998). While the Lower Ordovician strata are considerably more condensed in the Brunflo area than in Slemmestad, the difference is much less pronounced in the Middle Ordovician. The interval between 'Blommiga bladet' and the presumed position of 'Blodläget' is even more expanded in Brunflo than in Slemmestad. This possibly indicates that the identification of 'Blodläget' in Brunflo is incorrect. The confidence in the identification of 'Blodläget' in the Tingskullen core is much stronger. It is expressed as a heamatite impregnated surface and the biostratigraphical control, placing it at the base of *B. navis* is very strong (Wu et al. submitted).

8.4 Darriwilian

The Holen Limestone starts with a glauconitic grainstone bed with an erosional base. This level correlates with the thick packstone bed developed in the middle part of the rhythmites of the Lysaker Formation that marks the Volkhov-Kunda transition (Nielsen 1995), a level that has been associated with a brief sea level fall in Västergötland (Lindskog et al. 2014). This regression should be expressed also in the Tingskullen core, but detailed sedimentological data of this interval is lacking. At the outcrop at Byrum, northern Öland however, the Volkhov-Kunda boundary is likely represented by goethitic/limonitic ooids in middle of Formation A+B (cf. Stouge 2004). The Volkhov-Kunda boundary marks the start of a ~1.75 Myr long period of increased influx of meteorites which has been linked to a major breakup of a L-chondrite asteroid parent body at ~470 Ma (Schmitz et al. 2001). Strata of the *Lenodus variabilis*, *Yangtzeplacognathus crassus* and *Microzarkodina hagetiana* conodont zones are all enriched in chondrite grains (Schmitz et al. 2008).

The 'Täljsten' is a faunally and lithologically anomalous facies developed in the Kunda strata (approximately Dw1-2 boundary) of Västergötland, Sweden, where it is recognisable as an approximately 1.5 m thick grey interval in the otherwise red limestones (e.g. Mellgren & Eriksson 2009; Eriksson et al. 2012). The 'Täljsten' likely formed during a rapid regression-transgression cycle and marks a biotic turnover (Eriksson et al. 2012). The interval spans the transition between *Asaphus expansus* and *Asaphus raniceps* as well as *L. variabilis* and *Y. crassus*, in ascending order (Eriksson et al. 2012). The biostratigraphy and the anomalous facies suggest that the uppermost 0.3 m of the Svartodden Member correlates to the upper part of the 'Täljsten interval'.

The 'Täljsten' is marked by a rapid carbon isotope shift in the Gullhögen quarry of Västergötland (Meidla et al. 2004), a shift which can potentially be traced globally; the base of *Y. crassus* zone in Maocaopu and Puxi River, China documented by Schmitz et al. (2010), also coincides with a rapid isotope shift. A similar development can be seen in the interval between approx. -17 and -19 m in the Brunflo core, where the thicknesses of the limestone beds are thicker than both below and above and which is marked by a rapid shift in the carbon isotope curve. This shift is rapid and of minor magnitude, but both the decreasing and increasing trends are recorded by several samples and is therefore not an artefact. For these reasons the interval is interpreted as coeval with the 'Täljsten'. A similar development is seen between -28 and -30 m in the Tingskullen core, at the top of Formation A+B

(Wu et al. submitted).

As the inorganic carbon isotope data for the Slemmestad outcrops have been proven unreliable such a shift cannot be employed to recognise the 'Täljsten' in the Norwegian successions. The entire Svartodden Member in itself does correspond to the regression-transgression facies development however, and is thus correlated to the Täljsten in its entirety (cf. Kröger & Rasmussen 2014). Biostatigraphically, both the base of *A. raniceps* (Nielsen 1995) and the *Y. crassus* (Rasmussen et al. 2013; Kröger & Rasmussen 2014) zones begins in this member, though the exact positions are not pinpointed in any of the studies. The Svartodden Member is overlain by the Helskjer Member of the Elnes Formation, which would then represent the post-'Täljsten' transgression.

The interval that in the Brunflo core is represented by the upper member of the Holen Limestone as well as the Segerstad Limestone overlies the strata studied in Slemmestad. These sediments are likely coeval with the upper part of the Elnes Formation which has not been included in the present study.

9 Conclusions

The Tremadocian-Darriwilian outcrops of Bjerkåsholmen and Djuptrekkodden peninsulas near Slemmestad, Oslo and the Swedish Geological Survey's Brunflo #2 core were studied with respect to sedimentology and carbon isotope stratigraphy. These were compared to the core from Tingskullen, Öland described by Calner et al. (2014) and Wu et al. (submitted).

The correlation implies a similar sedimentation pattern throughout the western Baltoscandian basin during the studied interval, but the strata are more considerably more expanded in Tremadocian and Floian times in the Oslo area as compared to Jämtland and Öland. The palaeodepth was greatest in the Slemmestad area and most shallow in the Tingskullen core area. Brunflo represent an intermediate position.

The strata are, as a whole, extremely condensed, with average sedimentation rates of only a few millimetres per thousand years. Glauconite is an authigenic mineral forming at low sedimentation rates. The two beds of the Ceratopyge Limestone in Brunflo yield abundant glauconite, and the study shows that glauconony of the upper bed is more evolved, indicating a longer interval of non-deposition than for the lower bed.

Combining microfacies analysis and carbon isotope stratigraphy, several surfaces and intervals important for regional correlation have tentatively been identified for the first time in the Oslo-Asker area and at Brunflo. These include 'Blommiga bladet', 'Blodläget' as well as the regressive facies associated with the Volkhov-Kunda boundary and the subsequent 'Täljsten' interval. As the biostratigraphic control is stronger in the Oslo outcrop, the degree of confidence in the identifications is stronger here than within the Brunflo core.

Carbon isotope signatures have a great potential for both intrabasinal and global correlations. Several important carbon isotope excursions and trends of the Lower and Middle Ordovician can be recognised in the high resolution carbon isotope data from the Brunflo core. These include the LTNICE in the Latorp Limestone, the Floian-Darriwilian rise in the Latorp and Tøyen formations and the BDNICE in the basal part of the Lanna Limestone. A negative excursion is represented in the upper part of the lower member of the Holen Limestone. It immediately precedes the rising limb of the MDICE, which is clearly expressed in the upper member of the Holen and Segerstad limestones.

Caution should be exercised in the study of inorganic carbon isotope signatures for the Ordovician outcrops of the Oslo-Asker area as an significant overprint from the Caledonian Orogeny has disturbed the signal. The organic carbon signature is more stable and provides better data.

An extensive degree of recrystallisation and/or pseudomorphism recorded in the Bjørkåsholmen Formation, Latorp Limestone and Hagastrand Member indicate that evaporite conditions may have prevailed in Baltoscandia during the Lower Ordovician despite being positioned on relatively high latitudes. That sign of evaporitic conditions are not being found in the studied Middle Ordovician strata may be linked to climatic cooling (cf. Trotter et al. 2008). The onset of climatic cooling from the earlier prevailing greenhouse conditions may have caused increased biodiversity and the Great Ordovician Biodiversity Event and with that, increased burial of light organic carbon. This is reflected by the Floian-Darriwilian rise and the Middle-Darriwilian carbon isotope excursion, which have both been documented in the present study.

10 Acknowledgements

First and foremost, I would like to express my heartfelt gratitude to my supervisor Mikael Calner and co-supervisor Oliver Lehnert for introducing me to the project and for all the advice and encouragement you have provided me throughout the process of writing this thesis. Rongchang Wu and Niklas Brådenmark, I am grateful for all the help you have given me and all the fruitful discussions we have had. Git Klintvik Ahlberg and Anders Lindahl have been invaluable in the lab, with instruction and preparation of samples. I would also like to thank Leif Johansson, Carl Alwmark and Mats Eriksson for instructions on how to coat samples and operate the SEM. Anders Lindskog is thanked for the inspirational discussions, as are Per Ahlberg and Britta Smångs for help in locating bibliographical rareties and advice on reference management. Without the comradeship of the fellow students at Geocentrum, writing this thesis would not have been half as enjoyable. Lastly, I would like to thank my family for supporting me through all these years of study.

11 References

Ahlberg, P. 1988: Agnostid trilobites from the Ordovician of Jämtland, Sweden. *Geologiska Föreningens i Stockholm Förhandlingar 110*, 267–278.

Ainsaar, L., Kaljo, D., Martma, T., Männik, P., Nõlvak, J. & Tinn, O., 2010: Middle and Upper Ordovician carbon isotope chemostratigraphy in Baltoscandia: A correlation standard and clues to environmental history. *Palaeogeography, Palaeoclimatology, Palaeoecology 294*, 189–201.

Albanesi, G.L. & Bergström, S.M., 2004: Conodonts: Lower to Middle Ordovician record. *In* B.D. Webby, F. Paris, M.L. Droser & I.G. Percival (eds.): *The Great Ordovician Biodiversification Event*, 312–326. Columbia University Press, New York.

Amberg, C., Collart, T., Salenbien, W., Vandenbroucke, T.R.A., Egger, L.M., Munnecke, A., Nielsen, A.T., Hammer, Ø. & Verniers, J., 2013: The nature of Ordovician limestone-mudstone alternations in the Oslo-Asker area (Norway): Primary or diagenetic rythms? *In* A. Lindskog & K. Mehlquist (eds.): *Proceedings of the 3rd IGCP 591 Annual Meeting – Lund, Sweden, 9–19 June*, 25–26. Lund University, Lund.

Amorosi, A., 1995: Glaucony and sequence stratigraphy: a conceptual framework of distribution in siliciclastic sequences. *Journal of Sedimentary Research B65,* 419–425.

Amorosi, A., 1997: Detecting compositional, spatial, and temporal attributes of glaucony: a tool for provenance research. *Sedimentary Geology 109*, 135–153.

Antun, P., 1967: Sedimentary pyrite and its metamorphism in the Oslo Region. *NGT 47*, 211–235.

Balthasar, U.B. & Cusack, M., 2015: Aragonite-calcite seas–Quantifying the grey area. *Geology 43,* 99–102.

Barnes, C.R. 2004: Ordovician oceans and climate. *In* B.D. Webby, F. Paris, M.L. Droser & I.G. Percival (eds.): *The Great Ordovician Biodiversification Event*, 72–76. Columbia University Press, New York.

Bergström, S.M., 1980: Conodonts as paleotemperature tools in Ordovician rocks of the Caledonides and adjacent areas in Scandinavia and the British Isles. *Geologiska Föreningens i Stockholm Förhandlingar 102*, 377–392.

Bergström, S.M., Chen, X., Guitérrez-Marco, J.C. & Dronov, A., 2009: The new chronostratigraphic classification of the Ordovician System and its relations to major regional series and stages and to $\delta^{13}C$ chemostratigraphy. *Lethaia 42*, 97–107.

Bergström, S.M. & Löfgren, A., 2008: The base of the global Dapingian Stage (Ordovician) in Baltoscandia: conodonts, graptolites and unconformities. *Earth and Environmental Science Transactions of the Royal Society of Edinburgh 99*, 189–212.

Bjørlykke, K., 1974: Depositional history and geochemical composition of Lower Palaeozoic epicontinental sediments from the Oslo Region. *NGU Bulletin 305*, 1–81.

Bockelie, J.F., 1982: The Ordovician of Oslo-Asker. *In* D.L. Bruton & S.H. Williams (eds.): Field excursion guide. IV International Symposium on the Ordovician System. *Palaeontological Contributions from the University of Oslo 279*, 106–122.

Brøgger, W.C., 1882: *Die silurischen Etagen 2 und 3 im Kristianiagebiet und auf Eker.* Universitätsprogramm, Kristiania (Oslo). 376 pp.

Bruton, D.L., Gabrielsen, R.H. & Larsen, B.T., 2010: The Caledonides of the Oslo Region, Norway – stratigraphy and structural elements. *Norwegian Journal of Geology 90*, 93–121.

Bruton, D.L. & Willams, S.H., 1982 (eds.): Field excursion guide. IV International Symposium on the Ordovician System. *Palaeontological Contributions from the University of Oslo 279*, 1–217.

Burchette, T.P. & Wright, V.P., 1992: Carbonate ramp depositional systems. *Sedimentary Geology 79,* 3-57.

Calner, M., Erlström, M., Lehnert, O. & Ahlberg, P., 2013: Lower Palaeozoic geology of southern Sweden. *In* M. Calner, P. Ahlberg, O. Lehnert & M. Erlström (eds.): The Lower Palaeozoic of southern Sweden and the Oslo Region, Norway. Field Guide for the 3rd Annual Meeting of the IGCP project 591, 6–9. *Sveriges geologiska undersökning Rapporter och meddelanden 133*.

Calner, M., Lehnert, O., Wu, R., Dahlquist, P. & Joachimski, M.M., 2014: $\delta^{13}C$ chemostratigraphy in the Lower-Middle Ordovician succession of Öland (Sweden) and the global significance of the MDICE. *GFF 136*, 48–54.

Clauer, N., Keppens, E. & Stille, P., 1992: Sr isotopic constraints on the process of glauconitization. *Geology 20,* 133–136.

Cobbold, P.R., Zanella, A., Rodrigues, N. & Løseth, H., 2013: Bedding-parallel fibrous veins (beef and cone-in-cone): Worldwide occurrence and possible significance in terms of fluid overpressure, hydrocarbon generation and mineralization. *Marine and Petroleum Geology 43*, 1–20.

Cocks, L.R.M., 2001: Ordovician and Silurian global geography. *Journal of the Geological Society 158*, 197–210.

Cocks, L.R.M. & Torsvik, T.H., 2005: Baltica from the late Precambrian to mid-Palaeozoic times: The gain and loss of a terrane's identity. *Earth-Science Reviews 72*, 39–66.

Cooper, R.A. & Lindholm, K. 1990: A precise worldwide correlation of early Ordovician graptolite sequences. *Geological Magazine 127*, 497–525.

Cooper, R.A. & Sadler, P.M., 2012: The Ordovician Period. *In* F.M. Gradstein, J.G. Ogg & A.G. Smith (eds.): *A Geological Time Scale 2004*, 165–187. Cambridge University Press, Cambridge.

Demicco, R.V. & Hardie, L.A., 1994: Sedimentary Structures and Early Diagenetic Features of Shal-

low Marine Carbonate Deposits. *SEPM Atlas Series 1*, 1–256.

Dronov, A.V., Ainsaar, L., Kaljo, D., Meidla, T., Saadre, T. & Einasto, R., 2011: Ordovician of Baltoscandia: Facies, sequences and sea-level changes. *In* J.C. Gutiérrez-Marco, I. Rábano & D. García-Bellido (eds.): Ordovician of the World, 143–150. *Cuadernos del Museo Geominero 14*.

Dronov, A. & Holmer, E., 1999: Depositional sequences in the Ordovician of Baltoscandia. *Acta Universitatis Carolinae 43*, 133–136.

Droser, M.L. & Bottjer, D.J., 1986: A semiquantitative field classification of ichnofabric. *Journal of Sedimentary Petrology 56,* 558–559.

Dunham, R.J., 1962: Classification of carbonate rocks according to depositional texture. *AAPG Memoir 1*, 108–121.

Ebbestad, J.O.R., 1999: Trilobites of the Tremadoc Bjørkåsholmen Formation in the Oslo Region, Norway. *Fossils and Strata 47*, 1–118.

Egenhoff, S., Cassle, C., Maletz, J., Frisk, Å.M., Ebbestad, J.O.R. & Stübner, K., 2010: Sedimentology and sequence stratigraphy of a pronounced Early Ordovician sea-level fall on Baltica – The Bjørkåsholmen Formation in Norway and Sweden. *Sedimentary Geology 224*, 1–14.

Egenhoff, S. & Maletz, J., 2007: Graptolites as indicators of maximum flooding surfaces in monotonous deep-water shelf successions. *Palaios 22*, 373–383.

Egger, L.M., Amberg, C., Vandenbroucke, T.R.A., Munnecke, A., Salenbien, W., Collart, T., Nielsen, A.T. & Hammer, Ø, 2013: Primary or diagenetic rythms? Geochemical investigations on limestone-marl couplets from the Late Ordovician Skogerholmen Formation (Hovedøya Island, southern Norway). *In* A. Lindskog & K. Mehlquist (eds.): *Proceedings of the 3rd IGCP 591 Annual Meeting – Lund, Sweden, 9–19 June*, 90–92. Lund University, Lund.

Ekdale, A.A. & Bromley, R.G., 2001: Bioerosional innovation for living in carbonate hardgrounds in the Early Ordovician of Sweden. *Lethaia 34*, 1–12.

Erdtmann, B.-D., 1965: Outline stratigraphy of graptolite-bearing 3b (Lower Ordovician) strata in the Oslo Region, Norway. *Norsk Geologisk Tidsskrift 45*, 481–547.

Erdtmann, B.-D. & Paalits, I., 1994: The Early Ordovician "*Ceratopyge* Regressive Event" (CRE): Its correlation and biotic dynamic across the East European Platform. *Geologija 17*, 36–57.

Eriksson, M.E., Lindskog, A., Calner, M., Mellgren, J.I.S., Bergström, S.M., Terfelt, F. & Schmitz, B., 2012: Biotic dynamics and carbonate microfacies of the conspicuous Darriwilian (Middle Ordovician) 'Täljsten' interval, south-central Sweden. *Palaeogeography, Palaeoclimatology, Palaeoecology 367*, 89–103.

Fjelldahl, Ø., 1966: *The Ceratopyge Limestone (3aγ) and limestone facies in the Lower Didymograptus Shale 83b) in the Oslo Region and adjacent districts*. Cand. Real. thesis, University of Oslo, Norway,129 pp.

Flügel, E., 2010: *Microfacies of Carbonate Rocks. Analysis, Interpretation and Application*. Springer-Verlag, Berlin. 967 pp.

Gee, D.G., 1980: Basement-cover relationships in the central Scandinavian Caledonides. *Geologiska Föreningens i Stockholm Förhandlingar 102*, 455–474.

Guttormsen, J., 2012: *Sedimentology, palaeontology and diagenesis of the Ordovician (Darriwilian) Svartodden Member (Huk Formation), Slemmestad, Oslo Region*. M.Sc. thesis, University of Oslo, Norway, 174 pp.

Hammer, Ø., 2003: Biodiversity curves for the Ordovician of Baltoscandia. *Lethaia 36,* 305–314.

Hansen, T., 2009: Trilobites of the Middle Ordovician Elnes Formation of the Oslo Region, Norway. *Fossils and Strata 56*, 1–215.

Hansen, T., Nielsen, A.T. & Bruton, D.L., 2011: Palaeoecology in a mud-dominated epicontinental sea: A case study of the Ordovician Elnes Formation, southern Norway. *Palaeogeography, Palaeoclimatology, Palaeoecology 299,* 348–362.

Harper, D.A.T., 2006: The Ordovician biodiversification: Setting an agenda for marine life. *Palaeogeography, Palaeoclimatology, Palaeoecology 232*, 148–166.

Harris, M.T., Sheehan, P.M., Ainsaar, L., Hints, L., Männik, P., Nõlvak, J. & Rubel, M., 2004: Upper Ordovician sequences of western Estonia. *Palaeogeography, Palaeoclimatology, Palaeoecology 210,* 135–148.

Haq, B.U. & Shutter, S.R., 2008: A chronology of Paleozoic sea-level changes. *Science 322,* 64–68.

Hoel, O.A., 1999a: Trilobites of the Hagastrand Member (Tøyen Formation, lowermost Arenig) from the Oslo Region, Norway. Part I: Asaphidae. *Norsk Geologisk Tidsskrift 79*, 179–204.

Hoel, O.A., 1999b: Trilobites of the Hagastrand Member (Tøyen Formation, lowermost Arenig) from the Oslo Region, Norway. Part II: Remaining non-asaphid groups. *Norsk Geologisk Tidsskrift 79*, 259 –280.

Hugget, J.M., 2005: Minerals - Glauconites. *In* R.C. Selley, L.R.M. Cocks & I.R. Plimer (eds.): *Encyclopedia of geology*, 542–548. Elsevier, Amsterdam.

Jaanusson, V., 1960. The Viruan (Middle Ordovician) of Öland. *Bulletin of the Geological Institution of Uppsala University 38*, 207–288.

Jaanusson, V., 1972: Aspects of carbonate sedimentation in the Ordovician of Baltoscandia. *Lethaia 6*, 11–34.

Jaanusson, V. 1982: Introduction to the Ordovician of Sweden. *In* D.L. Bruton & S.H. Williams (eds.): Field excursion guide. IV International Symposium on the Ordovician System, 1–9. *Palaeontological Contributions from the University of Oslo 279*.

Jaanusson, V., 1984: What is so special about the Ordovician? *In* D.L. Bruton (ed.): Aspects of the Or-

dovician System, 1–3. *Palaeontological Contributions from the University of Oslo 295*.

Jaanusson, V., 1995: Confacies differentiation and upper Middle Ordovician correlation in the Baltoscandian basin. *Proceedings of the Estonian Academy of Sciences 44*, 73–86.

Jaanusson, V., Larsson, K. & Karis, L., 1982: The sequence in the Autochton of Jämtland. *In* D.L. Bruton & S.H. Williams (eds.): Field excursion guide. IV International Symposium on the Ordovician System, 55–63. *Palaeontological Contributions from the University of Oslo 279*.

Jianhua, Z. & Sturkell, E.F.F., 1998: Aserian and Lasnamägian (Middle Ordovician) conodont biostratigraphy and lithology at Kullstaberg and Lunne in Jämtland, central Sweden. *GFF 120*, 75–83.

Kaljo, D., Martma, T. & Saadre, T., 2007: Post-Hunnebergian Ordovician carbon isotope trend in Baltoscandia, its environmental implications and some similarities with that of Nevada. *Palaeogeography, Palaeoclimatology, Palaeoecology 245,* 138 –155.

Kanygin, A., Dronov, A., Timokhin, A. & Gonta, T., 2010: Depositional sequences and palaeoceanographic change in the Ordovician of the Siberian craton. *Palaeogeography, Palaeoclimatology, Palaeoecology 296,* 285–296.

Karis, L., 1998: Jämtlands östliga fjällberggrund. *In* L. Karis & A. Strömberg (eds.): Beskrivning till berggrundskartan över Jämtlands län. Del 2: Fjälldelen. *Sveriges geologiska undersökning Ca 53:2,* 6–178.

Karis, L. & Larsson, K., 1982: Jämtland road-log 2:4 – 4:2. *In* D.L. Bruton & S.H. Williams (eds.): Field excursion guide. IV International Symposium on the Ordovician System. *Palaeontological Contributions from the University of Oslo 279*, 64–76.

Kelly, J.C. & Webb, J.A., 1999: The genesis of glauconey in the Oligo-Miocene Torquay Group, southeastern Australia: petrographic and geochemical evidence. *Sedimentary Geology 125*, 99–114.

Kendall, A.C. & Harwood, G.M., 1996: Marine evaporites: arid shorelines and basins. *In* H.G. Reading (ed): *Sedimentary environments: Processes, Facies and Stratigraphy*, Blackwell Science, 281–324.

Kjerulf, T., 1857: *Über die Geologie des südlichen Norvegens.* Verlag von Johan Dahl, Christiania (Oslo). 141 pp.

Knauth, L.P. & Kennedy, M.J., 2009: The late Precambrian greening of the Earth. *Nature 460*, 728–732.

Kröger, B. & Rasmussen J.A., 2014: Middle Ordovician cephalopod biofacies and palaeoenvironments of Baltoscandia. *Lethaia 47*, 275–295.

Kump, L.R. & Arthur, M.A., 1999: Interpreting carbon -isotope excursions: carbonates and organic matter. *Chemical Geology 161*, 181–198.

Larsson, K., 1973: The lower Viruan in the autochthonous Ordovician sequence of Jämtland. *Sveriges Geologiska Undersökning C 683*, 1–82.

Lasemi, Z. & Sandberg, P.A., 1984: Transformation of aragonite-dominated lime muds to microcrystalline limestones. *Geology 12*, 420–423.

Lehnert, O., Meinhold, G., Wu, R.-C., Calner, M., Joachimski, M.M., 2014: $\delta^{13}C$ chemostratigraphy in the upper Tremadocian through lower Katian (Ordovician) carbonate succession of the Siljan district, central Sweden. *Estonian Journal of Earth Sciences 63*, 277–286.

Lidmar-Bergström, K., 1993: Denudation surfaces and tectonics in the southernmost part of the Baltic Shield. *Precambrian Research 64*, 337–345.

Lidmar-Bergström, K., 1995: Relief and saprolites through time on the Baltic shield. *Geomorphology 12*, 45–61.

Lindholm, K., 1991: Hunnebergian graptolites and biostratigraphy in southern Scandinavia. *Lund Publications in Geology 95*, 1–36.

Lindskog, A., Eriksson, M.E. & Pettersson, A.M.L., 2014: The Volkhov-Kunda transition and the base of the Holen Limestone at Kinnekulle, Västergötland, Sweden. *GFF 136*, 167–171.

Lindström, M., 1979: Diagenesis of Lower Ordovician hardgrounds in Sweden. *Geologica et Palaeontologica 13*, 9–30.

Löfgren, A., 1978: Arenigian and Llanvirnian conodonts from Jämtland, northern Sweden. *Fossils and Strata 13*, 1–129.

Meidla, T., Ainsaar, L., Backman, J., Dronov, A., Holmer, L. & Sturesson, U., 2004: Middle–Upper Ordovician carbon isotopic record from Västergötland (Sweden) and East Baltic. *In* O. Hints & L. Ainsaar (eds.): *WOGOGOB-2004 Conference Materials*, 67–68. Tartu University Press, Tartu.

Mellgren, J.I.S. & Eriksson, M.E., 2009: Untangling a Darriwilian (Middle Ordovician) palaeoecological event in Baltoscandia: conodont faunal changes across the 'Täljsten' interval. *Earth and Environmental Science Transactions of the Royal Society of Edinburgh 100*, 353–370.

Munnecke, A., 1997: Bildung mikritischer Kalke im Silur auf Gotland. *Courier Forschungsinstitut Senckenberg 198*, 1–131.

Munnecke, A., Calner, M., Harper, D.A.T. & Servais, T., 2010: Ordovician and Silurian sea-water chemistry, sea level, and climate: A synopsis. *Palaeogeography, Palaeoclimatology, Palaeoecology 296,* 389–413.

Munnecke, A. & Samtleben, C., 1996: The formation of micritic limestones and the development of limestone-marl alternations in the Silurian of Gotland, Sweden. *Facies 34*, 159–176.

Munnecke, A., Westphal, H., Elrick, M. & Reijmer, J.J.G., 2001: The mineralogical composition of precursor sediments of calcareous rhythmites: a new approach. *International Journal of Earth Sciences 90*, 795–812.

Nakrem, H.A. & Rasmussen, J.A., 2013: Oslo Region, Norway. *In* M. Calner, P. Ahlberg, O. Lehnert & M. Erlström (eds.): The Lower Palaeozoic of southern Sweden and the Oslo Region, Norway. Field

Guide for the 3rd Annual Meeting of the IGCP project 591, 58–66. *Sveriges geologiska undersökning Rapporter och meddelanden 133*.

Nicoll, R.S., Laurie, J.R., Shergold, J.H. & Nielsen, A.T., 1992: Preliminary correlation of latest Cambrian to Early Ordovician sea level events in Australia and Scandinavia. *In* B.D. Webby & J.R. Laurie (eds.): *Global Perspectives on Ordovician Geology*, 381–394. A.A. Balkema, Rotterdam.

Nielsen, A.T., 1995: Trilobite systematics, biostratigraphy and palaeoecology of the Lower Ordovician Komstad Limestone and Huk Formations, southern Scandinavia. *Fossils and Strata 38*, 1–374.

Nielsen, A.T., 2004: Ordovician sea level changes: A Baltoscandian perspective. *In* B.D. Webby, F. Paris, M.L. Droser & I.G. Percival (eds.): *The Great Ordovician Biodiversification Event*, 84–93. Columbia University Press, New York.

Nielsen, A.T. & Schovsbo, N.H., 2007: Cambrian to basal Ordovician lithostratigraphy in southern Scandinavia. *Bulletin of the Geological Society of Denmark 53*, 47–92.

Nielsen, A.T. & Schovsbo, N.H., 2013: The Cambo-Ordovician Alum Shale revisited: Depositional environment, sea-level changes and transient isostatic disturbances. *In* A. Lindskog & K. Mehlquist (eds.): *Proceedings of the 3rd IGCP 591 Annual Meeting – Lund, Sweden, 9–19 June*, 249–251. Lund University, Lund.

Odin, G.S. (ed.) 1988: Green Marine Clays – Oolitic Ironstone Facies, Verdine Facies, Glaucony Facies and Celadonite-Bearing Facies – A Comparative Study. *Developments in Sedimentology 45*, 1–445.

Odin, G.S. & Fullagar, P.D., 1988: Geological significance of the glaucony facies. *In* G.S. Odin (ed.): Green Marine Clays – Oolitic Ironstone Facies, Verdine Facies, Glaucony Facies and Celadonite-Bearing Facies – A Comparative Study, 295–332.

Odin, G.S. & Matter, A., 1981: De glauconarium origine. *Sedimentology 28,* 611–641.

Owen, A.W., Bruton, D.L., Bockelie, J.F. & Bockelie, T.G., 1990: The Ordovician successions of the Oslo Region, Norway. *Norges geologiske undersøkelse Special Publication 4*, 3–54.

Palmer, T.J. & Wilson, M.A., 2004: Calcite precipitation and dissolution of biogenic aragonite in shallow Ordovician calcite seas. *Lethaia 37*, 417–427.

Pärnaste, H., Bergström, J. & Zhiyi, Z., 2013: High resolution trilobite stratigraphy of the Lower–Middle Ordovician Öland Series of Baltoscandia. *Geological Magazine 150*, 509–518.

Rasmussen, J.A., 1991: Conodont stratigraphy of the Lower Ordovician Huk Formation at Slemmestad, southern Norway. *Norsk Geologisk Tidsskrift 71*, 265–288.

Rasmussen, J.A., 2001: Conodont biostratigraphy and taxonomy of the Ordovician shelf margin deposits in the Scandinavian Caledonides. *Fossils and Strata 48*, 1–180.

Rasmussen, J.A., Bruton, D.L. & Nakrem, H.A., 2013: Tremadocian to Darriwilian units, Bjørkåsholmen and Djuptrekkodden, Slemmestad. *In* M. Calner, P. Ahlberg, O. Lehnert & M. Erlström (eds.): The Lower Palaeozoic of southern Sweden and the Oslo Region, Norway. Field Guide for the 3rd Annual Meeting of the IGCP project 591, 67–72. *Sveriges geologiska undersökning Rapporter och meddelanden 133*.

Reyment, R.A., 1968: Orthoconic nautiloids as indicators of shoreline surface currents. *Journal of Sedimentary Petrology 38*, 1387–1389.

Ross, C.A. & Ross, J.R.P., 1995: North American Ordovician depositional sequences and correlations. *In* J.D. Cooper, M.L. Droser & S.C. Finney (eds.): Ordovician Odyssey: Short Papers for the Seventh International Symposium on the Ordovician System, 309 – 313. *Pacific Section Society for Sedimentary Geology (SEPM) Book 77*.

Ross, J.R.P. & Ross, C.A., 1992: Ordovician sea-level fluctuations. *In* B.D. Webby & J.R. Laurie (eds.): *Global Perspectives on Ordovician Geology*, 327–335. A.A. Balkema, Rotterdam.

Saltzman, M.R. & Thomas, E., 2012: Carbon isotope stratigraphy. *In* F.M. Gradstein, J.G. Ogg, M.D. Schmitz & G.M. Ogg (eds.): *The Geologic Time Scale*, 207–232. Elsevier, Amsterdam.

Schmitz, B., Bergström, S.M. & Xiaofeng, W., 2010: The middle Darriwilian (Ordovician) $\delta^{13}C$ excursion (MDICE) discovered in the Yangtze Platform succession in China: implications of its first recorded occurrences outside Baltoscandia. *Journal of the Geological Society 167*, 249–259.

Schmitz, B., Harper, D.A.T., Peucker-Ehrenbrink, B., Stouge, S., Alwmark, C., Cronholm, A., Bergström, S.M., Tassinari, M. & Xiaofeng, W., 2008: Asteroid breakup linked to the Great Ordovician Biodiversification Event. *Nature Geoscience 1*, 49–53.

Schmitz, B., Tassinari, M. & Peucker-Ehrenbrink, B., 2001: A rain of ordinary chondritic meteorites in the early Ordovician. *Earth and Planetary Science Letters 194*, 1–15.

Scholle, P.A. & Ulmer-Scholle, D.S., 2003: A Color Guide to the Petrography of Carbonate Rocks: Grains, Textures, Porosity, Diagenesis. *AAPG Memoir 77*, 1–474.

Sepkoski, J.J.Jr., 1981: A factor analytic description of the Phanerozoic marine fossil record. *Paleobiology 7*, 36–53.

Størmer, L., 1953: The Middle Ordovician of the Oslo Region, Norway, 1. Introduction to stratigraphy. *Norsk Geologisk Tidsskrift 31*, 37–141.

Stouge, S., 2004: Ordovician siliciclastics and carbonates of Öland, Sweden. *Erlanger geologische Abhandlungen Sonderband 5*, 91–111.

Sturkell, E., 1991: Tremadocian Ceratopyge Limestone identified by means of conodonts, in Jämtland, Sweden. *GFF 113*, 185–188.

Su, W., 2007: Ordovician sea-level changes: evidence from the Yangtze Platform. *Acta Palaeontologica*

Sinica 46 (suppl.), 471–476.
Tjernvik, T.E., 1956: On the Early Ordovician of Sweden – stratigraphy and fauna. *Bulletin of the Geological Institution of Uppsala 36*, 107–284.
Trotter, J.A., Williams, I.S., Barnes, C.R., Lécuyer, C. & Nicoll, R.S., 2008: Did cooling oceans trigger Ordovician biodiversification? Evidence from conodont thermometry. *Science 321*, 550–554.
Tucker, M.E., 2001: *Sedimentary Petrology*. Blackwell Publishing, Malden. 262 pp.
Webby, B.D., Paris, F., Droser, M.L. & Percival, I.G. (eds.) 2004: *The Great Ordovician Biodiversification Event*. Columbia University Press, New York. 484 pp.
Westphal, H., 2006: Limestone-marl alternations as environmental archives and the role of early diagenesis: a critical review. *International Journal of Earth Sciences 95*, 947–961.
Wickström, L.M., 2007: Ordovician of the Storsjön area. *In* J.O. Ebbestad, L. Wickström, & A. Högström (eds.): WOGOGOB 2007. 9th Meeting of the Working Group on Ordovician Geology of Baltoscandia, Field guide and Abstracts, 41–44. *Sveriges geologiska undersökning Rapporter och meddelanden 128.*
Wilson, M.A. & Palmer, T.J., 2001: The Ordovician Bioerosion Revolution. *Geological Society of America Abstracts With Programs 33,* 248.
Wilson, M.A. & Palmer, T.J., 2006: Patterns and processes in the Ordovician Bioerosion Revolution. *Ichnos 13*, 109–112.
Wright, V.P. & Burchette, T.P., 1998: Carbonate ramps: an introduction. *In* V.P. Wright & T.P. Burchette (eds.): Carbonate Ramps. *Geological Society, London, Special Publications 149*, 1–5.
Wu, R.-C., Calner, M. & Lehnert, O., submitted: Integrated conodont biostratigraphy and carbon isotope chemostratigraphy in the Lower–Middle Ordovician of southern Sweden.
Wu, R.-C., Calner, M., Lehnert, O., Peterffy, O. & Joachimski, J.J., in press: Lower–Middle Ordovician $\delta^{13}C$ chemostratigraphy of western Baltica (Jämtland, Sweden). *Palaeoworld* doi:10.1016/j.palwor.2015.01.003
Wu, Y. & Wu, Z., 1996: Two-phase diagenetic alteration of carbonate matrix: Middle Ordovician limestones, Taiyuan City area, China. *Sedimentary Geology 106*, 177–191.
Young, S.A., Saltzman, M.R., Bergström, S.M., Leslie, S.A. & Xu, C., 2008: Paired $\delta^{13}C_{carb}$ and $\delta^{13}C_{org}$ records of Upper Ordovician (Sandbian–Katian) carbonates in North America and China : Implications for paleoceanographic change. *Palaeogeography, Palaeoclimatology, Palaeoecology 270,* 166–178.
Zhang, T., Shen, Y. & Algeo, T.J., 2010: High-resolution carbon isotopic records from the Ordovician of South China: Links to climatic cooling and the Great Ordovician Biodiversification Event (GOBE). *Palaeogeography, Palaeoclimatology, Palaeoecology 289,* 102–112.

Tidigare skrifter i serien ”Examensarbeten i Geologi vid Lunds universitet”:

378. Åkesson, Sofia, 2014: Skjutbanors påverkan på mark och miljö. (15 hp)
379. Härling, Jesper, 2014: Food partitioning and dietary habits of mosasaurs (Reptilia, Mosasauridae) from the Campanian (Upper Cretaceous) of the Kristianstad Basin, southern Sweden. (45 hp)
380. Kristensson, Johan, 2014: Ordovicium i Fågelsångskärnan-2, Skåne – stratigrafi och faciesvariationer. (15 hp)
381. Höglund, Ida, 2014: Hiatus - Sveriges första sällskapsspel i sedimentologi. (15 hp)
382. Malmer, Edit, 2014: Vulkanism - en fara för vår hälsa? (15 hp)
383. Stamsnijder, Joaen, 2014: Bestämning av kvartshalt i sandprov - metodutveckling med OSL-, SEM– och EDS-analys. (15 hp)
384. Helmfrid, Annelie, 2014: Konceptuell modell över spridningsvägar för glasbruksföroreningar i Rejmyre samhälle. (15 hp)
385. Adolfsson, Max, 2014: Visualizing the volcanic history of the Kaapvaal Craton using ArcGIS. (15 hp)
386. Hajny, Casandra, 2014: Ett mystiskt ryggradsdjursfossil från Åsen och dess koppling till den skånska, krittida ryggradsdjursfaunan. (15 hp)
387. Ekström, Elin, 2014: – Geologins betydelse för geotekniker i Skåne. (15 hp)
388. Thuresson, Emma, 2014: Systematisk sammanställning av större geoenergianläggningar i Sverige. (15 hp)
389. Redmo, Malin, 2014: Paleontologiska och impaktrelaterade studier av ett anomalt lerlager i Schweiz. (15 hp)
390. Artursson, Christopher, 2014: Comparison of radionuclide-based solar reconstructions and sunspot observations the last 2000 years. (15 hp)
391. Svahn, Fredrika, 2014: Traces of impact in crystalline rock – A summary of processes and products of shock metamorphism in crystalline rock with focus on planar deformation features in feldspars. (15 hp)
392. Järvin, Sara, 2014: Studie av faktorer som påverkar skredutbredningen vid Norsälven, Värmland. (15 hp)
393. Åberg, Gisela, 2014: Stratigrafin i Hanöbukten under senaste glaciationen: en studie av borrkärnor från IODP’s expedition nr 347. (15 hp)
394. Westlund, Kristian, 2014: Geomorphological evidence for an ongoing transgression on northwestern Svalbard. (15 hp)
395. Rooth, Richard, 2014: Uppföljning av utlastningsgrad vid Dannemora gruva; april 2012 - april 2014. (15 hp)
396. Persson, Daniel, 2014: Miljögeologisk undersökning av deponin vid Getabjär, Sölvesborg. (15 hp)
397. Jennerheim, Jessica, 2014: Undersökning av långsiktiga effekter på mark och grundvatten vid infiltration av lakvatten – fältundersökning och utvärdering av förhållanden vid Kejsarkullens avfallsanläggning, Hultsfred. (15 hp)
398. Särman, Kim, 2014: Utvärdering av befintliga vattenskyddsområden i Sverige. (15 hp)
399. Tuvesson, Henrik, 2014: Från hav till land – en beskrivning av geologin i Skrylle. (15 hp)
400. Nilsson Brunlid, Anette, 2014: Paleoekologisk och kemisk-fysikalisk undersökning av ett avvikande sedimentlager i Barsebäcks mosse, sydvästra Skåne, bil dat för ca 13 000 år sedan. (15 hp)
401. Falkenhaug, Jorunn, 2014: Vattnets kretslopp i området vid Lilla Klåveröd: ett kunskapsprojekt med vatten i fokus. (15 hp)
402. Heingård, Miriam, 2014: Long bone and vertebral microanatomy and osteohistology of ’Platecarpus’ ptychodon (Reptilia, Mosasauridae) – implications for marine adaptations. (15 hp)
403. Kall, Christoffer, 2014: Microscopic echinoderm remains from the Darriwilian (Middle Ordovician) of Västergötland, Sweden – faunal composition and applicability as environmental proxies. (15 hp)
404. Preis Bergdahl, Daniel, 2014: Geoenergi för växthusjordbruk – Möjlig anläggning av värme och kyla i Västskåne. (15 hp)
405. Jakobsson, Mikael, 2014: Geophysical characterization and petrographic analysis of cap and reservoir rocks within the Lund Sandstone in Kyrkheddinge. (15 hp)
406. Björnfors, Oliver, 2014: A comparison of size fractions in faunal assemblages of deep-water benthic foraminifera—A case study from the coast of SW-Africa.. (15 hp)

407. Rådman, Johan, 2014: U-Pb baddeleyite geochronology and geochemistry of the White Mfolozi Dyke Swarm: unravelling the complexities of 2.70-2.66 Ga dyke swarms on the eastern Kaapvaal Craton, South Africa. (45 hp)
408. Andersson, Monica, 2014: Drumliner vid moderna glaciärer — hur vanliga är de? (15 hp)
409. Olsenius, Björn, 2014: Vinderosion, sanddrift och markanvändning på Kristianstadsslätten. (15 hp)
410. Bokhari Friberg, Yasmin, 2014: Oxygen isotopes in corals and their use as proxies for El Niño. (15 hp)
411. Fullerton, Wayne, 2014: REE mineralisation and metasomatic alteration in the Olserum metasediments. (45 hp)
412. Mekhaldi, Florian, 2014: The cosmic-ray events around AD 775 and AD 993 - Assessing their causes and possible effects on climate. (45 hp)
413. Timms Eliasson, Isabelle, 2014: Is it possible to reconstruct local presence of pine on bogs during the Holocene based on pollen data? A study based on surface and stratigraphical samples from three bogs in southern Sweden. (45 hp)
414. Hjulström, Joakim, 2014: Bortforsling av kaxblandat vatten från borrningar via dagvattenledningar: Riskanalys, karaktärisering av kaxvatten och reningsmetoder. (45 hp)
415. Fredrich, Birgit, 2014: Metadolerites as quantitative P-T markers for Sveconorwegian metamorphism, SW Sweden. (45 hp)
416. Alebouyeh Semami, Farnaz, 2014: U-Pb geochronology of the Tsineng dyke swarm and paleomagnetism of the Hartley Basalt, South Africa – evidence for two separate magmatic events at 1.93-1.92 and 1.88-1.84 Ga in the Kalahari craton. (45 hp)
417. Reiche, Sophie, 2014: Ascertaining the lithological boundaries of the Yoldia Sea of the Baltic Sea – a geochemical approach. (45 hp)
418. Mroczek, Robert, 2014: Microscopic shock-metamorphic features in crystalline bedrock: A comparison between shocked and unshocked granite from the Siljan impact structure. (15 hp)
419. Balija, Fisnik, 2014: Radon ett samhällsproblem - En litteraturstudie om geologiskt sammanhang, hälsoeffekter och möjliga lösningar. (15 hp)
420. Andersson, Sandra, 2014: Undersökning av kalciumkarbonatförekomsten i infiltrationsområdet i Sydvattens vattenverk, Vombverket. (15 hp)
421. Martin, Ellinor, 2014: Chrome spinel grains from the Komstad Limestone Formation, Killeröd, southern Sweden: A high-resolution study of an increased meteorite flux in the Middle Ordovician. (45 hp)
422. Gabrielsson, Johan, 2014: A study over Mg/Ca in benthic foraminifera sampled across a large salinity gradient. (45 hp)
423. Ingvaldson, Ola, 2015: Ansvarsutredningar av tre potentiellt förorenade fastigheter i Helsingborgs stad. (15 hp)
424. Robygd, Joakim, 2015: Geochemical and palaeomagnetic characteristics of a Swedish Holocene sediment sequence from Lake Storsjön, Jämtland. (45 hp)
425. Larsson, Måns, 2015: Geofysiska undersökningsmetoder för geoenergisystem. (15 hp)
426. Hertzman, Hanna, 2015: Pharmaceuticals in groundwater - a literature review. (15 hp)
427. Thulin Olander, Henric, 2015: A contribution to the knowledge of Fårö's hydrogeology. (45 hp)
428. Peterffy, Olof, 2015: Sedimentology and carbon isotope stratigraphy of Lower–Middle Ordovician successions of Slemmestad (Oslo-Asker, Norway) and Brunflo (Jämtland, Sweden). (45 hp)

LUNDS UNIVERSITET

Geologiska institutionen
Lunds universitet
Sölvegatan 12, 223 62 Lund